



**SCC and Crevice corrosion inhibition of Steam Turbine ASTM A470 Steel  
(3.5 Ni -1Cr - 1Mo - 0.25V) and 7050-T74 Al-alloys  
using VpCI 337 and Ecoline 3690**

**Prepared for:**

**CORTEC Corp.**

Prepared by:

Behzad Bavarian, Jia Zhang and Lisa Reiner  
Dept. of Manufacturing Systems Engineering & Management  
College of Engineering and Computer Science  
California State University, Northridge  
Northridge, CA 91330

March 2011

Stress corrosion cracking and crevice corrosion of Steam Turbine: ASTM A470 (3.5Ni -1Cr - 1Mo - 0.25V), and 7050-T74 Al-alloys were studied in the VpCI 337 and Ecoline 3690 Cortec products using the slow strain rate technique ASTM G129 and ASTM G48/C44 standards. The objective of this project is to investigate the VpCI 337 and Ecoline 3690 products contribution to corrosion inhibition of these alloys.

The program objectives are as follows:

- to study electrochemical behavior (cyclic polarization and EIS) of these alloys in different solutions with different concentration of V<sub>p</sub>CI 337 and Ecoline 3690 and different Cl<sup>-</sup> concentrations.
- to study the environmentally-assisted cracking susceptibility of samples prepared from these alloys
- to investigate the effectiveness of VCI inhibitors to stop corrosion attack in Cl<sup>-</sup>-containing solution under artificial crevices.

### **ABSTRACT**

The accumulation of damage due to localized corrosion, pitting, stress corrosion cracking and corrosion fatigue, in low pressure steam turbines components, such as blades, discs and rotors, has been consistently identified as being among the main causes of turbine failure. Accordingly, the development of effective localized corrosion inhibitors is essential for the successful avoidance of unscheduled downtime in steam turbines or other complex industrial and infrastructural systems and for the successful implementation of life extension strategies. Stress corrosion cracking of 7050 aluminum alloys and ASTM A470 steel in the turbo-expander and steam/gas turbines industry can cause expensive catastrophic failures, especially in those turbo-machinery systems performing in hostile corrosive environments. Commercially available inhibitors were investigated for their effectiveness in reducing and controlling the corrosion susceptibility.

Inhibitor effectiveness of VCI 337 and Ecoline 3690 products was confirmed with DC electrochemical corrosion techniques and EIS in different concentrations of inhibitor solutions. Polarization resistance increased with concentration of corrosion inhibitor due to film formation and displacement of water molecules. Cyclic polarization behavior for samples in the 1.0% and 5.0% inhibitors showed a shift in the passive film breakdown potential indicating more protective films. The substantial increase in the passivation range has favorable consequences for neutralizing pitting and crevice corrosion cell chemistry. The strain to failure and tensile strength from the slow strain rate stress corrosion cracking studies for both alloys showed pronounced effects of corrosion inhibition in the environment to retard SCC; the fractographic analysis showed a changed morphology with ductile overload as the primary failure mode instead of transgranular or intergranular cracking.

## INTRODUCTION

The accumulation of damage due to localized corrosion (pitting, stress corrosion cracking [SCC] and corrosion fatigue [CF]) in low pressure steam turbines components, such as blades, discs and rotors, has been consistently identified as being among the main causes of turbine failures [1, 2]. Accordingly, the development of effective localized corrosion inhibitors are essential for the successful avoidance of unscheduled downtime in steam turbines or other complex industrial and infrastructural systems and for the successful implementation of life extension strategies. The majority of damages occur during the shutdown period due to chemistry changes and stagnant conditions in localized areas. The environmental changes during the shutdown period are one of the main contributing environmental factors that determine the probability of blade and disc failure in low pressure steam turbines.  $[O_2]$ ,  $[Cl^-]$ , temperature, pH, and time spent under aerated conditions during the shutdown period increase the likelihood of localized corrosion attack. Increase in  $[Cl^-]$  concentration and pH changes affect the stability of the protective oxides and eventually its breakdown pitting, stress corrosion cracking and corrosion fatigue.

In general, it is believed that by lowering  $[Cl^-]$  below 35 ppm the susceptibility to localized corrosion decreases significantly. If chloride concentration on the surfaces is reduced immediately upon shutdown, this will provide a corrective strategy for minimizing or even eliminating the failure of disc and blades. This is most easily accomplished by washing the blade and disc surfaces with chloride-free water immediately upon shutdown of the turbine. In fact, an even more effective strategy would be to combine turbine surface washing with dehumidification or nitrogen blanketing. For the accessible surfaces, this strategy can work, but for the restricted geometries such as crevice, notch and cavities, to reach these surfaces is very difficult and dangerous to assume they have been washed. Accumulation of corrosive species and pH changes inside these restricted geometries can alter the electrochemical reactions to initiate pitting or crevice corrosion that eventually leads to stress corrosion cracking and corrosion fatigue.

Low pressure rotors are typically constructed of forgings conforming to ASTM A470, 3.5NiCrMoV (class 2 to 7). While shrunk-on disks are made of ASTM A 471 (class 1 to 3). The strength and hardness of turbine components must be limited because the stronger and harder materials become very susceptible to SCC and CF, particularly turbine rotors, discs and blades cannot be made of high strength materials. The crack propagation rate increases with yield strength and SCC becomes susceptible to hydrogen embrittlement. This susceptibility limits use of high strength materials for turbine discs in power plants (yield strength below 140 ksi, 965 MPa is recommended). However, in the turbo-machinery, the common impeller and turbine are 7xxx high strength aluminum alloys, mainly 7050 forged aluminum alloys. Some of the main reasons for selecting this alloy for turbine applications are light weight, toughness and corrosion resistance. However, residual stresses induced by the heat treatment in conjunction with those from the machining process make these materials sensitive to SCC. To improve SCC and CF resistance, this alloy is used in -T74 tempered condition. In either case of ASTM A470 or 7050-T74, corrosion protection is extremely critical to maintain functionality of these systems.

### **Vapor phase corrosion inhibitors**

Several groups of organic compounds have reported corrosion inhibiting effects for different alloys. The extent of adsorption of an inhibitor depends on many factors: (a) the nature and the surface charge of the metal; (b) the inhibitor adsorption mode; and (c) the inhibitor's chemical structure. The presence of heteroatoms (oxygen, nitrogen, sulfur, phosphorus), triple bonds and aromatic rings in the inhibitor's chemical structure enhance the adsorption process [9]. Coating to substrate adhesion and the diffusion of water and other species from an external environment to the coating/substrate interface are critical factors for the corrosion inhibition of organic protective coatings. One possibility for turbine materials protection is Volatile Corrosion Inhibitors (VCI), where protective vapors deposit on the exposed surfaces (including cracks and crevices) and condense to form a thin barrier of tiny crystals. The crystals dissolve when in contact with water, causing the adsorption of a monomolecular coating to the metal surface that helps repel water. VCI can also neutralize the pH and other corrosive species, which is an effective way to adjust the localized chemistry inside a crevice, pit or crack.

VCI is often a complex mixture of amine salts and aromatic sulfonic acids that provide direct contact inhibition and incorporate volatile carboxylic acid salts as a vapor phase inhibitor for metal surfaces not sufficiently coated. The thin polar layer of surfactants is tightly bound to the metal surface through chemisorption. Between this thin polar layer and the corrosive environment is the thicker barrier layer of hydrocarbons. The sulfonate part of the inhibitor displaces water from the metal surface and promotes chemisorption of inhibitor to the surface. A surface active inhibitor component will be strongly chemisorbed or adsorbed to the surface [7]. Active sites having energy levels complementary to the energy levels of the polar group, thereby forming a tighter, more uniform layer over the metal surface. The barrier layer has three important characteristics: 1) low permeability by moisture and other corrosives; 2) compatibility with the oleophilic ends of the polar layer molecules so that the barrier is held firmly in place; and 3) good solubility in the carrier to attach the polar and barrier layers to the metal surface [8]. The VCI film barrier replenishes through further evaporation and condensation of the inhibitor on the metal surface.

### **Turbo-machinery maintenance**

Turbo-machinery systems have regular service maintenance and unexpected shut downs. During these scheduled service maintenance, components are frequently washed to dilute or remove any in service contaminants (salt, dirt, grease and oil). There are three main types of cleaning: aqueous, organic solvent and abrasive. Aqueous cleaning covers a wide variety of cleaning methods (detergents, acids and alkaline compounds) to displace soil. Improved corrosion prevention compounds and coating systems can isolate the sensitive alloy from the environment. These coatings, combined with improved repair and maintenance procedures, will ensure adequate performance of a structure manufactured from a SCC sensitive alloy. The most costly, yet best method for eliminating SCC is to replace the material with an alloy specifically designed to resist this form of corrosion. The proposed inhibitors investigated in this program are heavy duty, biodegradable, water based alkaline cleaners and degreasers. The compounds function by altering hydrocarbons (grease) so that the deposits can be removed with water. Any conventional equipment (power washers, steam cleaners, dip tanks) can be used for multi-metal corrosion protection. Ethoxylated alcohols, the active ingredient in the inhibitor are based on short chain alcohols giving fast penetration of soil and improved performance on hard surfaces.

### Adsorption Isotherm Models

An adsorption isotherm is a mathematical function that relates the surface coverage of a chemical on a surface (usually a metal) to the concentration of the chemical. Identification of the surface adsorption isotherm is important in that it and classical thermodynamics can lead to the determination of a mechanism. It is assumed that the corrosion current density, which is directly related to the corrosion rate, is representative of the number of corrosion sites. Therefore, adding inhibitor to the environment should diminish the number of corrosion initiation sites by displacing water molecules on the surface with inhibitor molecules, thereby decreasing the corrosion rate. By measuring the corrosion current density of a solution with no inhibitor (blank) and an inhibited solution (or by measuring the polarization resistance), the surface coverage,  $\theta$ , can be defined by the following formula:

$$\theta = \frac{I_{corr}(B) - I_{corr}(I)}{I_{corr}(B)} \quad \text{or} \quad \theta = \frac{\frac{1}{Rp(B)} - \frac{1}{Rp(I)}}{\frac{1}{Rp(B)}} \Rightarrow \theta = \frac{Rp(I) - Rp(B)}{Rp(I)} \quad (1)$$

where  $I_{corr}(B)$  and  $Rp(B)$  are the corrosion current and polarization resistance of the blank solution, respectively.  $I_{corr}(I)$  and  $Rp(I)$  are the corrosion current and polarization resistance for the inhibited solution, respectively. In recent years, electrochemical and weight loss methods that relate the corrosion current density or the amount of weight loss with the inhibitor coverage have been used to study adsorption and the corrosion inhibition of various materials on a metallic surface [5, 6]. Many models for adsorption isotherms have been defined (Temkin, Freundlich, Langmuir and Frumkin). Each of these adsorption isotherms explains a different type of relationship between concentration and surface coverage of an inhibitor on a metal or alloy surface [7]. Based on the adsorption isotherm graph, the adsorption equilibrium constant,  $K_{ad}$ , can be calculated. Having the adsorption equilibrium constant, can lead to the calculation of the free standard energy of adsorption,  $\Delta G_{ad} = -RT \ln(K_{ad})$ . By repeating the same experiment at different temperatures, the enthalpy of the adsorption,  $\Delta H_{ad}$  can be calculated.

### EXPERIMENTAL PROCEDURES

Corrosion inhibition of VCI 337 and Ecoline 3690 were investigated for 7050 aluminum alloys and ASTM A470 steel in the turbo-expander and steam/gas turbines industry. ASTM A470 is common steel for low pressure steam turbine disc/rotor. Its chemical composition consist of 3.5% Ni -1.5%Cr – 0.8 %Mo - 0.25%V. The samples for investigation were annealed for 24 hrs and air cooled, hardness of 32 RC was achieved after heat treatment. 7050 Aluminum alloy is 6.5% Zn, 2%Mg and 2%Cu that was used in –T74 temper condition and hardness was 82-84 RB, while electrical conductivity was 38 IACS%.

Electrochemical polarization per ASTM-G61 standards was used to evaluate the electrochemical behavior of these inhibitors on the ASTM A470 steel and 7050 aluminum alloy. These techniques can provide useful information regarding the corrosion mechanisms, corrosion rate and localized corrosion susceptibility of the material for a given environment. The studies were conducted using a Gamry PC4/750™ Potentiostat/Galvanostat/ZRA and DC105 corrosion test

software. These alloys were tested in a solution of 1.0% and 5.0% inhibitor with 200 ppm Cl<sup>-</sup>. A series of cyclic polarization tests were performed in temperatures ranging from 20 °C to 50 °C. These tests were performed to investigate the effect of temperature on the VCI/metal behavior. For the cyclic polarization tests, samples were polished (600 grit sandpaper) placed in a flat cell and tested in different inhibitor concentrations of deionized water and 200 ppm Cl<sup>-</sup> solutions.

A Gamry PC4/750<sup>TM</sup> Potentiostat/Galvanostat/ZRA with electrochemical impedance spectroscopy (EIS300<sup>TM</sup>) software was used to further investigate the inhibitor effectiveness on these alloys and gather data for adsorption isotherms in different inhibitor concentrations of deionized water plus 200 ppm Cl<sup>-</sup>. Electrochemical impedance was measured by applying a sinusoidal signal to an electrochemical cell and measuring the current. The R<sub>p</sub> value (determined from the Bode plot) was used to fit the data into adsorption isotherm models.

**Table 1:** Cyclic polarization (ASTM G61) and EIS (ASTM G106) Corrosion Tests on ASTM A470 (3.5Ni - 1Cr - 1Mo - 0.25V) and 7050 Al-alloys in different solutions of V<sub>p</sub>CI 337 and Ecoline 3690.

<u>Environment</u>	<u>Inhibitor Concentration, %</u>	<u># of Tests each alloy</u>
water	0.0	4
water +200 ppm Cl <sup>-</sup>	0.0	4
water	1.0	4
water +200 ppm Cl <sup>-</sup>	1.0	4
water	5.0	4
water +200 ppm Cl <sup>-</sup>	5.0	4

### **Crevice Corrosion Investigation**

Both ASTM A470 and 7050 aluminum alloys were tested in an eight-station alternate immersion system. The samples were immersed in various concentrations of corrosion inhibitor, sodium chloride (Cl<sup>-</sup>) and tap water. Alternate immersion, an aggressive procedure, was performed to evaluate the inhibitor's ability to resist crevice corrosion. The testing cycle immersed the samples for 10 minutes, then exposed them to air for 50 minutes per ASTM G44 and G47. After 200 cycles of testing, the samples were disassembled, examined and photographed to document crevice corrosion resistance.

**Table 2:** Crevice Corrosion Tests on ASTM A470 (3.5Ni - 1Cr - 1Mo - 0.25V) and 7050 Al-alloys using artificial crevice samples in different solutions, alternate immersion test ASTM G48 and ASTM G44.

<u>Environment</u>	<u>V<sub>p</sub>CI 337 Concentration, %</u>	<u># of Tests each alloy</u>
water	0.0	2
water +200 ppm Cl <sup>-</sup>	0.0	2
water	1.0	2
water +200 ppm Cl <sup>-</sup>	1.0	2
water	5.0	2
water +200 ppm Cl <sup>-</sup>	5.0	2

**Table 3:** Crevice Corrosion Tests on ASTM A470 (3.5Ni-1Cr - 1Mo - 0.25V) and 7050 Al-alloys using artificial crevice samples in different solutions, alternate immersion test ASTM G48 and ASTM G44.

Environment	Ecoline 3690 Concentration,	# of Tests each alloy
water	0.0	2
water +200 ppm Cl-	0.0	2
water	coated	2
water +200 ppm Cl-	coated	2

### SCC Investigation

The slow strain rate tests were conducted on cylindrical samples under controlled electrochemical conditions using a strain rate of  $5 \times 10^{-7} \text{ sec}^{-1}$ . To evaluate the inhibitor's effectiveness, these alloys were tested in a 1.0 and 5.0% VCI solution (a typical concentration recommended to retard localized corrosion attack) and the reference samples were tested in tap water and +200 ppm Cl- solutions without inhibitor. To determine the degree of inhibitor effectiveness, anodic potentials of -400 mV<sub>sce</sub> (for 7050 Al-alloy) and -200 mV<sub>sce</sub> were applied to the samples during the test. These potential are close to the passive film breakdown potentials for these alloys, and are the most critical range of potential to initiate localized corrosion. Twenty four tests per alloy were completed to assess the degree of SCC susceptibility of each alloy in different solutions.

**Table 4:** SCC Corrosion Tests on ASTM A470 (3.5Ni -1Cr - 1Mo - 0.25V) and 7050 Al-alloys using the slow strain rate techniques in different solutions, Strain Rate =  $5 \times 10^{-7} \text{ sec}^{-1}$ .

Environment	V <sub>p</sub> CI 337 Concentration, %	# of Tests each alloy
water	0.0	2
water +200 ppm Cl-	0.0	2
water	1.0	2
water +200 ppm Cl-	1.0	2
water	5.0	2
water +200 ppm Cl-	5.0	2

**Table 5:** SCC Corrosion Tests on ASTM A470 (3.5Ni -1Cr - 1Mo - 0.25V) and 7050 Al-alloys using the slow strain rate techniques in different solutions, Strain Rate =  $5 \times 10^{-7} \text{ sec}^{-1}$ .

Environment	Ecoline 3690 Concentration	# of Tests each alloy
water	0.0	2
water +200 ppm Cl-	0.0	2
water	coated	2
water +200 ppm Cl-	coated	2



## RESULTS

### Cyclic Polarization Behavior

Figures 1-4 and Tables 6-8 show the polarization behavior for both alloys in different solutions. Most noticeable changes are the positive shift in the breakdown potentials by more than +500 mV for these alloys in the VpCI 337 inhibitor solutions. The inhibitor altered the electrochemistry, increased the passivation range significantly, and had beneficial consequences for reducing localized corrosion. As demonstrated in these polarization curves, extension of the passive zone contributes to the stability of the protective oxide film over a wider electrochemical range, resulting in a more stable passive film.

**Table 6** - Electrochemical behavior of ASTM A470 in 200 ppm Cl<sup>-</sup> & 1.0 or 5.0% VpCI 337 Solutions

Sample	Ec	Ic	Eb	CR	Passive range	Ipss
	mVsce	uA/cm <sup>2</sup>	mVsce	mpy	mVsce	uA/cm <sup>2</sup>
Water +0.0%VCI	-605	0.607	-300	0.26	none	NA
Water +1.0%VCI	-192	0.124	1450	0.05	-50 to +1230	1.77
200ppm Cl <sup>-</sup> +0.0%VCI	-675	1.47	-450	1.63	none	NA
200ppm Cl <sup>-</sup> +1.0%VCI	-460	0.389	+45	0.17	-300 to +20	3.12
200ppm Cl <sup>-</sup> +5.0%VCI	-415	0.228	240	0.10	-210 to +200	3.08

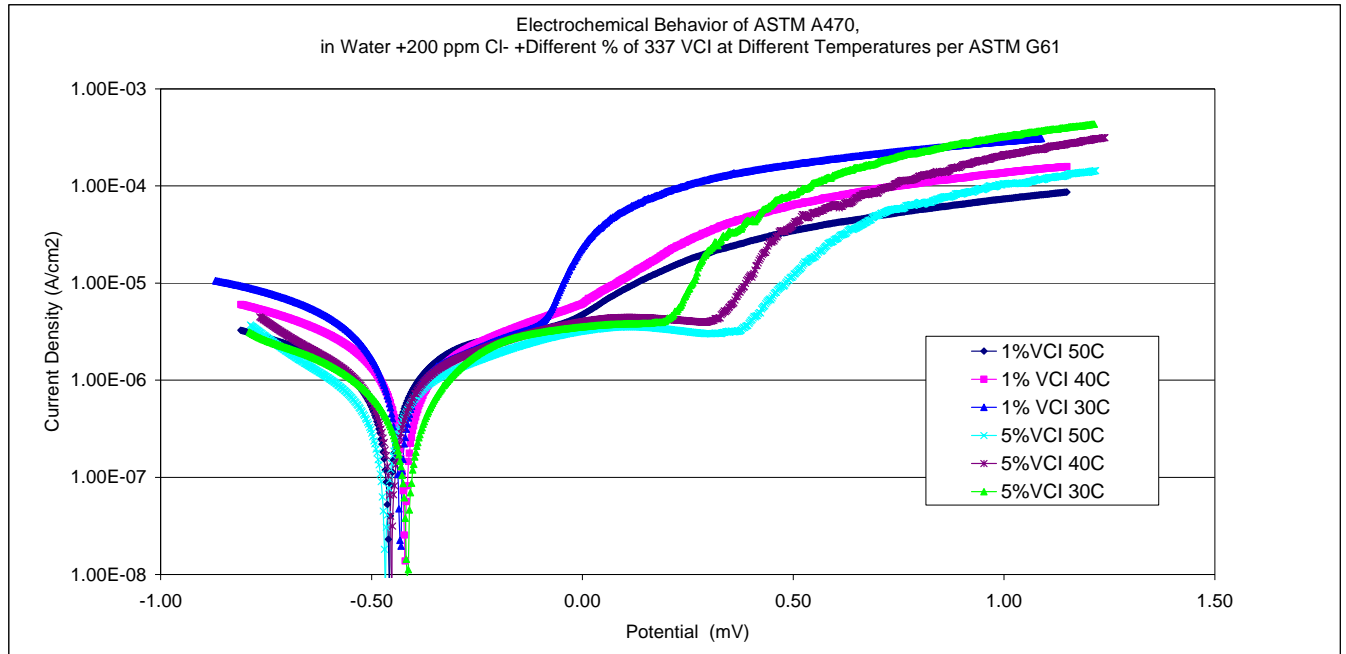
**Table 7** - Effects of temperature on electrochemical behavior of ASTM A470 in 200 ppm Cl<sup>-</sup> & 1.0 or 5.0% VCI Solution.

Sample	Temp	Ec	Ic	Eb	CR	Passive range	Ipss
	°C	mVsce	uA/cm <sup>2</sup>	mVsce	mpy	mVsce	uA/cm <sup>2</sup>
200ppm Cl <sup>-</sup> +0.0%VCI	30	-675	1.47	-450	0.63	none	NA
200ppm Cl <sup>-</sup> +1.0%VCI	30	-460	0.389	+45	0.17	-300 to +20	3.12
200ppm Cl <sup>-</sup> +1.0%VCI	40	-415	0.492	+70	0.21	-300 to +75	3.82
200ppm Cl <sup>-</sup> +1.0%VCI	50	-430	0.463	+130	0.20	-300 to +120	2.47
200ppm Cl <sup>-</sup> +5.0%VCI	30	-415	0.304	+240	0.12	-200 to +200	3.57
200ppm Cl <sup>-</sup> +5.0%VCI	40	-450	0.31	+320	0.13	-200 to +300	4.20
200ppm Cl <sup>-</sup> +5.0%VCI	50	-460	0.221	+430	0.09	-200 to +420	3.02

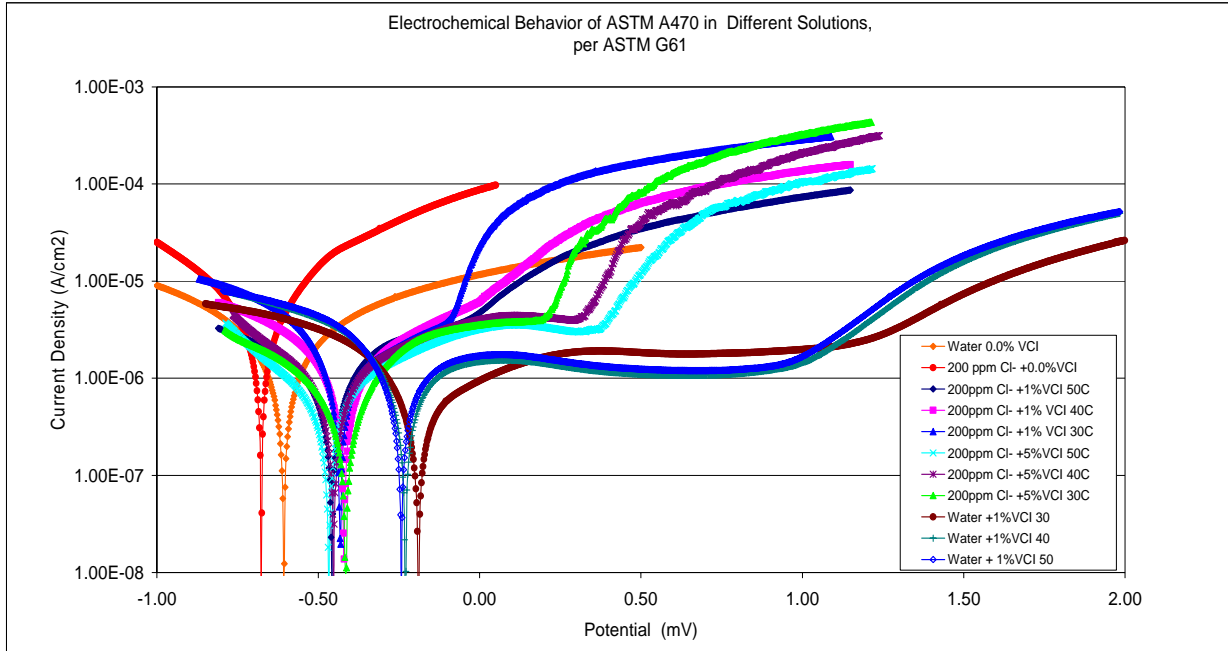


**Table 8** - Effects of temperature on electrochemical behavior of 7050-T74 Al-alloy in 200 ppm Cl<sup>-</sup> & 1.0 or 5.0% VCI Solution.

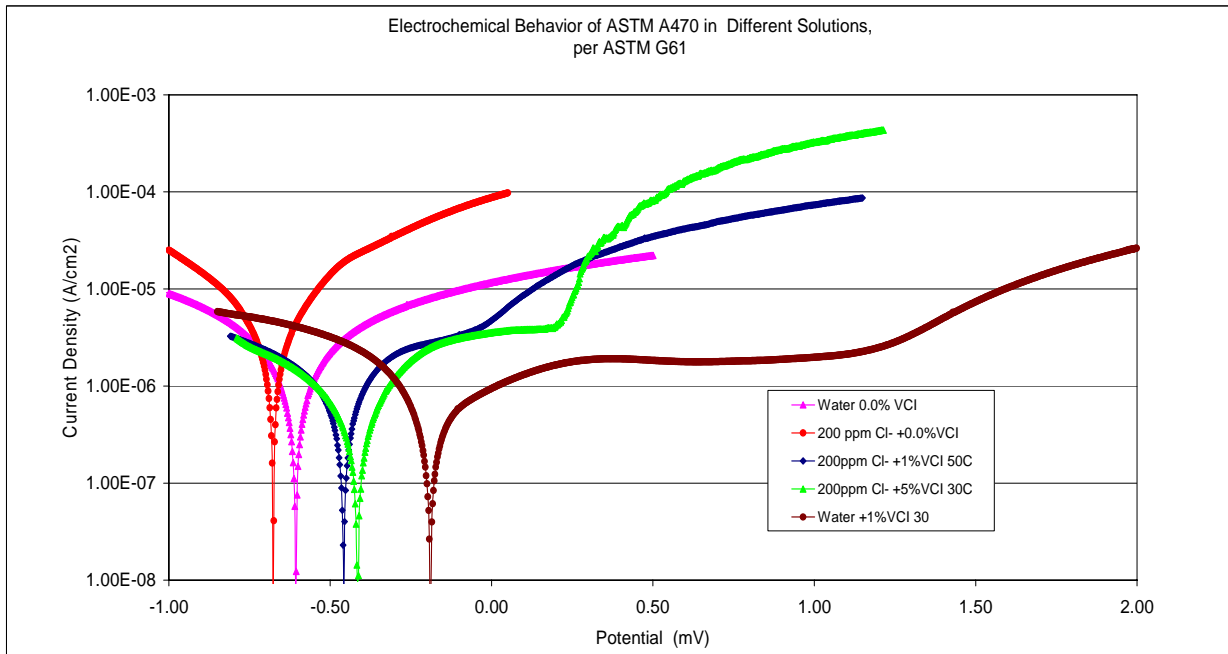
Sample	Temp	E <sub>c</sub>	I <sub>c</sub>	E <sub>b</sub>	CR	Passive range	I <sub>pss</sub>
	°C	mVsce	uA/cm <sup>2</sup>	mVsce	mpy	mVsce	uA/cm <sup>2</sup>
200ppm Cl <sup>-</sup> +0.0%VCI	30	-782	2.560	-700	1.13	none	NA
200ppm Cl <sup>-</sup> +1.0%VCI	30	-848	0.310	-510	0.14	-750 to -500	2.45
200ppm Cl <sup>-</sup> +1.0%VCI	40	-830	0.227	-500	0.10	-750 to -500	2.44
200ppm Cl <sup>-</sup> +1.0%VCI	50	-825	0.265	-455	0.12	-750 to -500	2.35
200ppm Cl <sup>-</sup> +5.0%VCI	30	-860	0.177	-300	0.08	-800 to -430	2.55
200ppm Cl <sup>-</sup> +5.0%VCI	40	-870	0.168	-318	0.07	-800 to -400	2.45
200ppm Cl <sup>-</sup> +5.0%VCI	50	-875	0.178	-330	0.08	-800 to -330	2.65



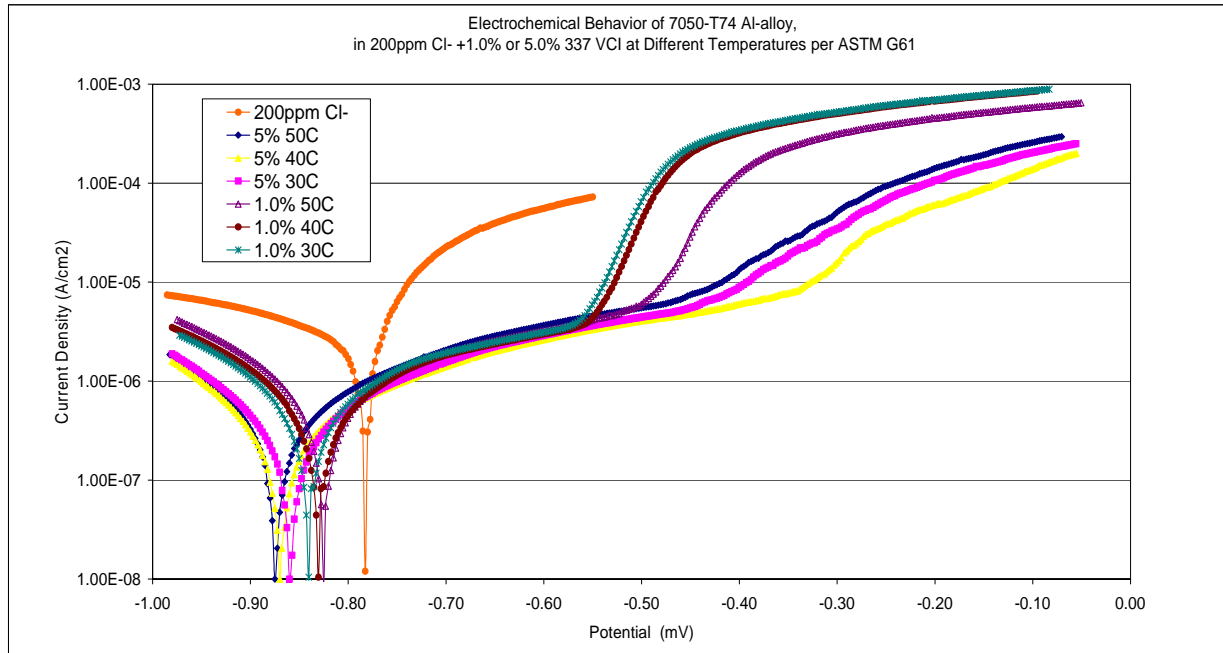
**Figure 1:** Electrochemical polarization behavior of ASTM A470 steel in different percent V<sub>p</sub>CI 337 solutions.



**Figure 2:** Effects of temperature on the electrochemical polarization behavior of ASTM A470 in different percent  $V_p$ CI 337 solution.



**Figure 3:** Electrochemical polarization behavior of ASTM A470 in different percent  $V_p$ CI 337 solution.



**Figure 4:** Effects of temperature on the electrochemical polarization behavior of 7050-T74 Al-alloy in different percent  $V_p$ CI 337 solution.

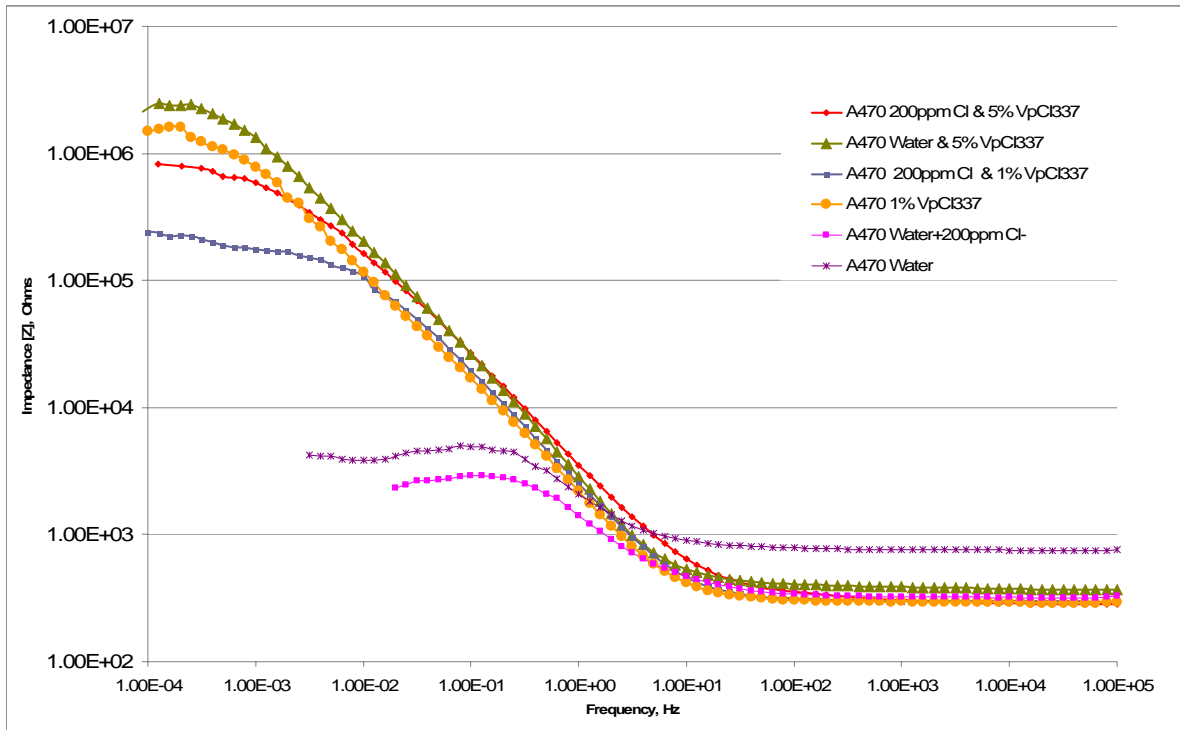
Electrochemical impedance spectroscopy, EIS (ASTM G106) test results are summarized in Tables 9-11 and Figures 5-11.  $V_p$ CI 337 inhibitor increased the resistance polarization. The increased polarization resistance can be attributed to the film formation on the metal surfaces and neutralizing of corrosive species. However, it appears that the  $V_p$ CI 337 inhibitor is more protective on ASTM A470 steel. Similar inhibition effectiveness was observed for Ecoline 3690 inhibitor (Table 11 and Figure 11). The  $R_p$  values for Ecoline 3690 inhibitor are very sensitive to film thickness. It was observed that a thicker inhibitor film resulted in very high resistance polarization value.

**Table 9:**  $R_p$  values (Kohms) for ASTM A470 aluminum alloys generated by EIS in water + inhibitors.

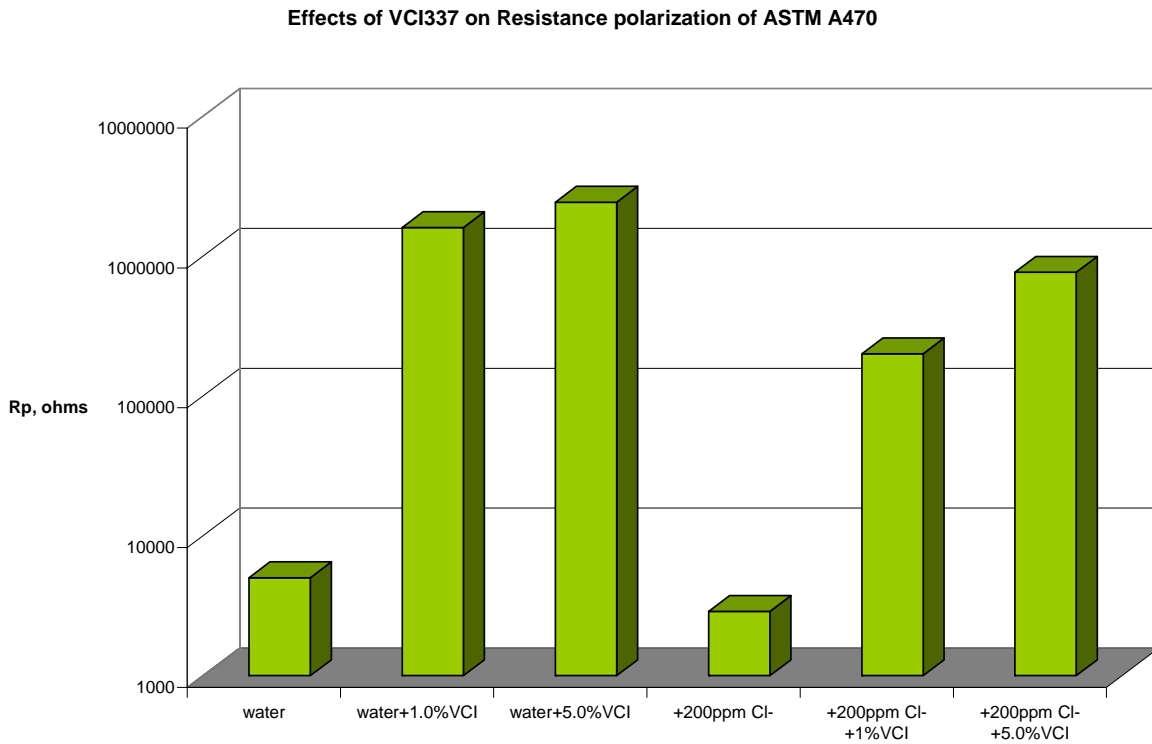
Alloy	$V_p$ CI 337 Concentration (%)		
	0.0%	1.0% VCI	5.0% VCI
ASTM A470	5.01	1,600	2,430
7050-T74	10.1	227	512

**Table 10:**  $R_p$  values (Kohms) for ASTM A470 and 7050 aluminum alloys generated by EIS in +200ppm  $Cl^-$  and inhibitors.

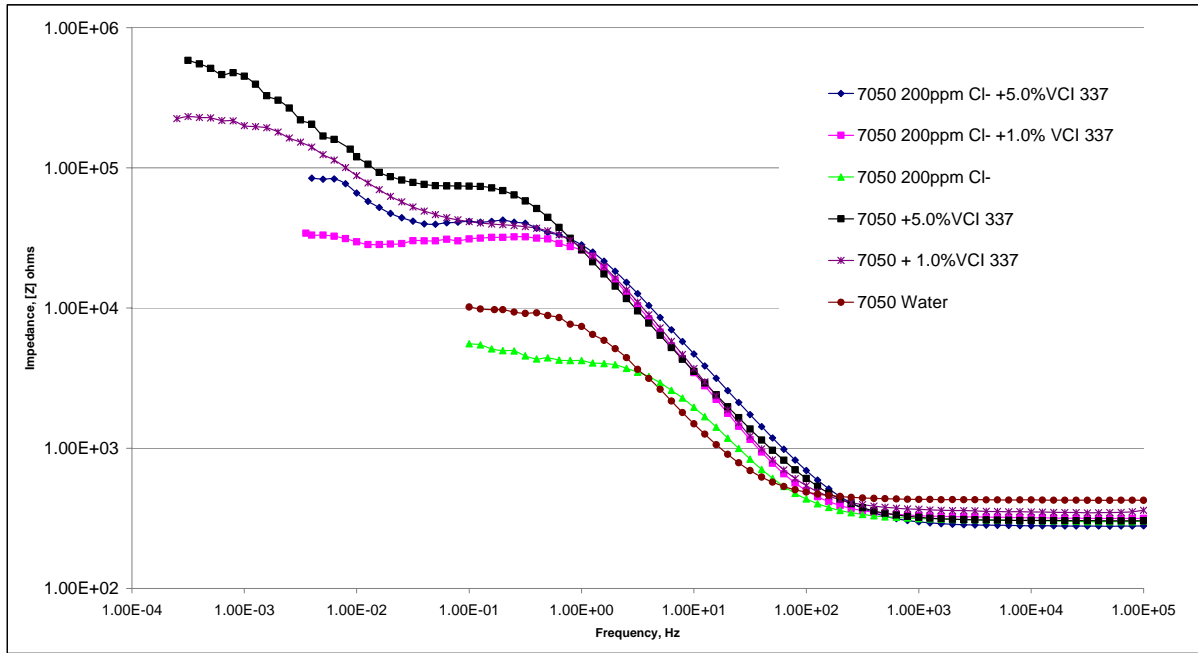
Alloy	$V_p$ CI 337 Concentration (%)		
	0.0%	1.0%VCI	5.0%VCI
ASTM A470	2.8	220	766
7050-T74	5.4	28.8	83.1



**Figure 5:** Electrochemical Impedance spectroscopy Bode plots of ASTM A470 steel in different solutions and different inhibitor concentrations.

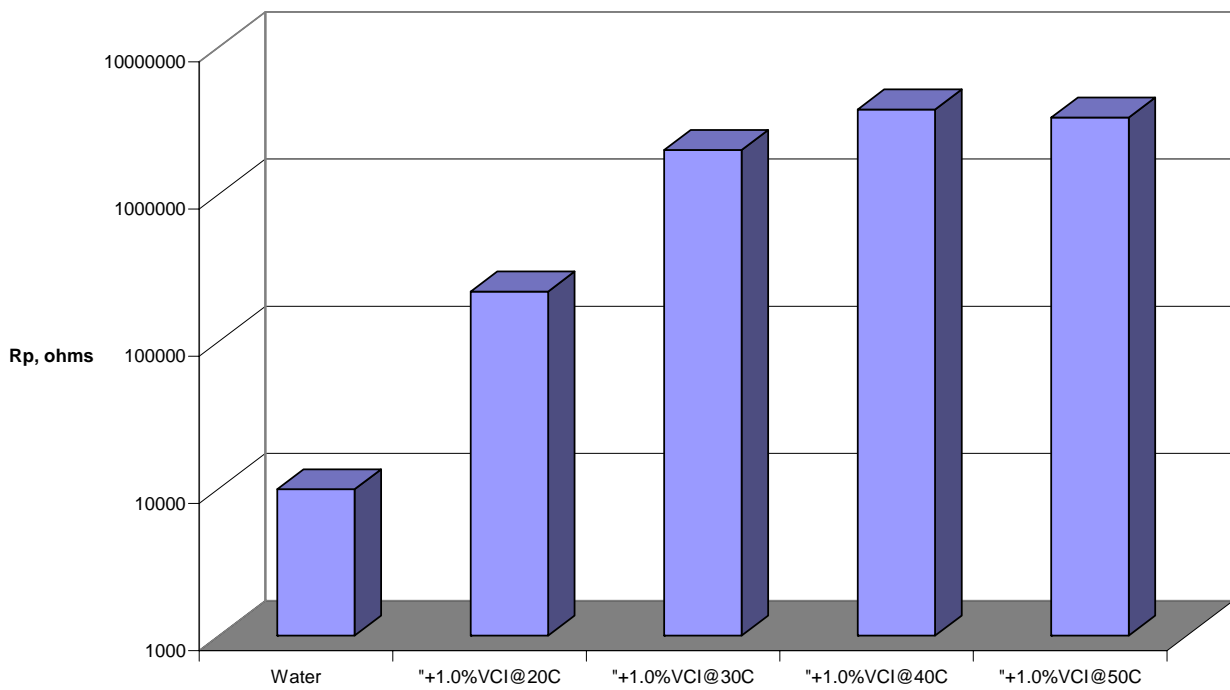


**Figure 6:** Summary of the Rp value for ASTM A470 in V<sub>p</sub>CI 337.

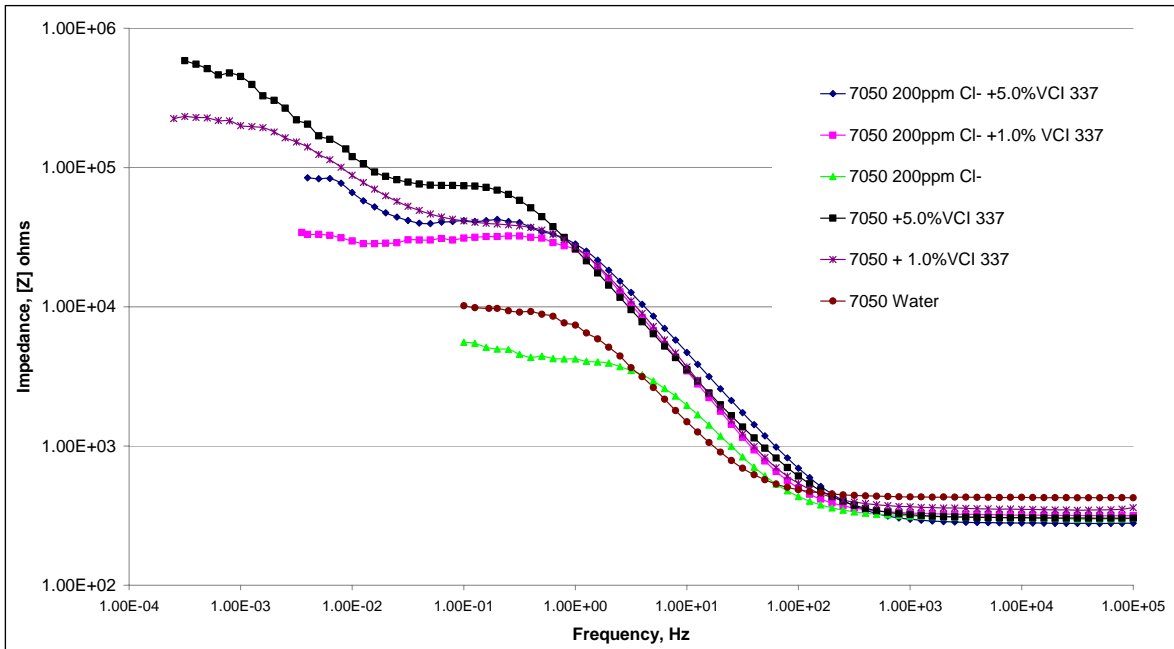


**Figure 7:** Electrochemical Impedance spectroscopy Nyquist plots of 7050-T74 alloy in various concentrations of inhibitor at different temperatures.

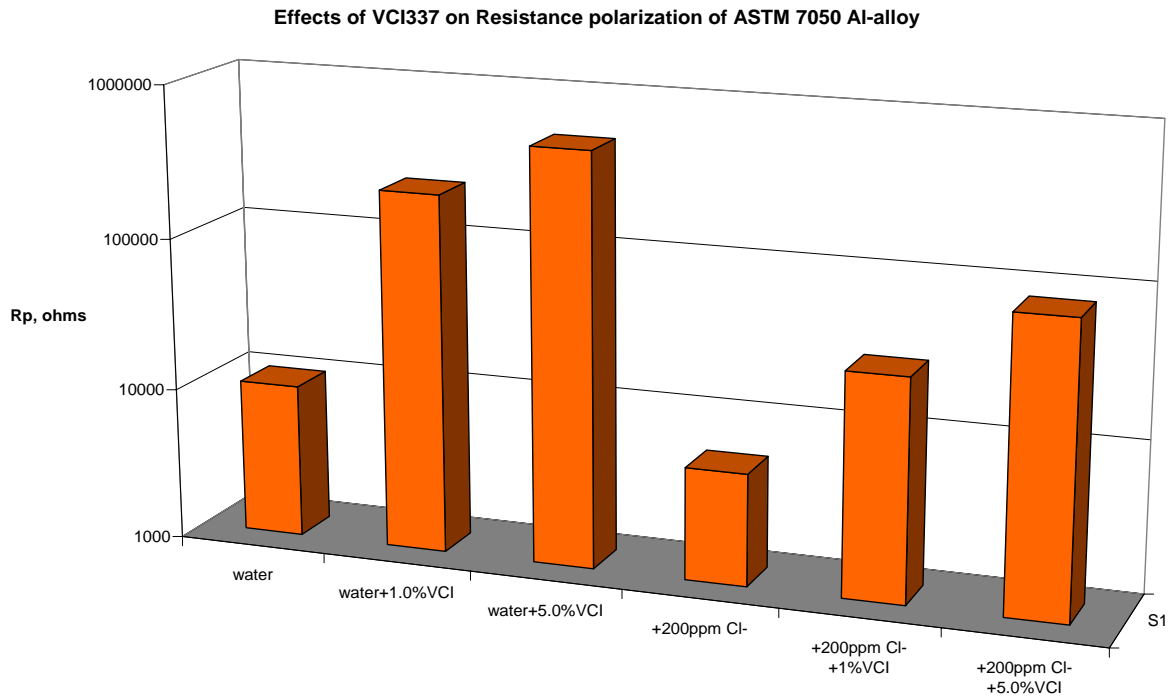
**Effects of VCI337 on Resistance polarization of 7050Al-alloy**



**Figure 8:** Summary of the Rp value for ASTM A470 in VpCI 337.



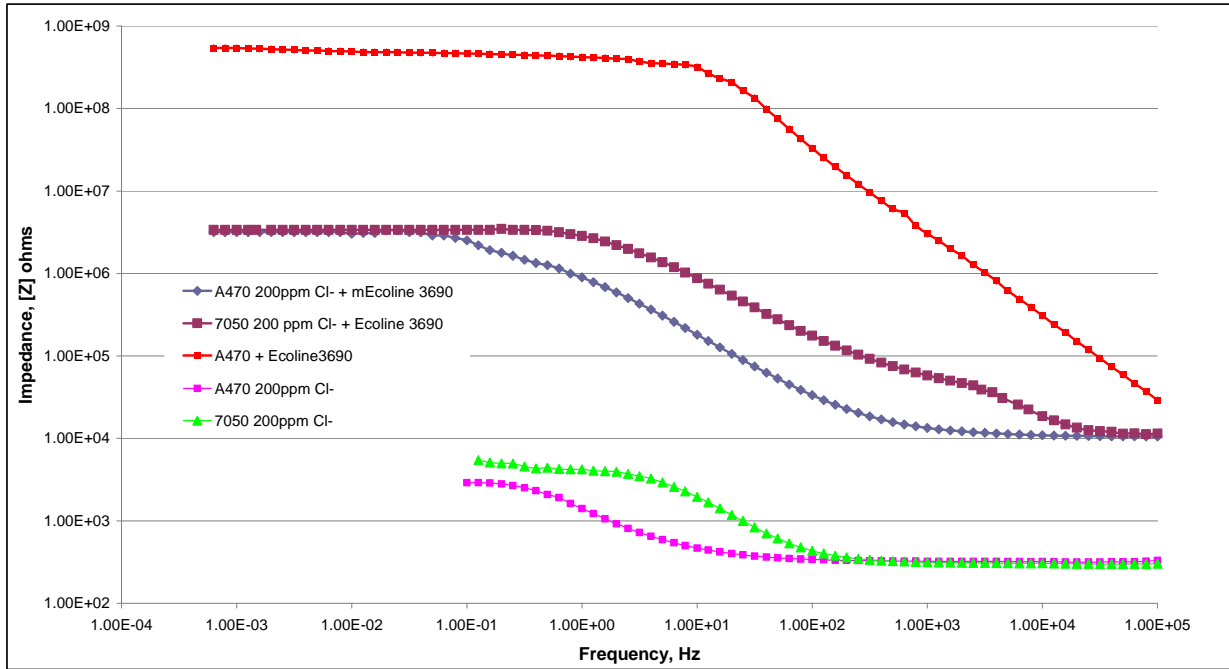
**Figure 9:** Electrochemical Impedance spectroscopy Bode plots of 7050-T74 alloy in various concentrations of  $V_p$ CI 337 inhibitor.



**Figure 10:** Summary of the  $R_p$  value for 7050 Al-alloy in  $V_p$ CI 337 inhibitor.

**Table 11:** Rp values (Kohms) for ASTM A470 and 7050 aluminum alloys generated by EIS in +200ppm Cl<sup>-</sup> coated with Ecoline 3690 inhibitor.

Alloy	Non-coated	Coated
ASTM A470	2.8	$3.4 \times 10^3$
7050-T74	5.4	$4.1 \times 10^3$




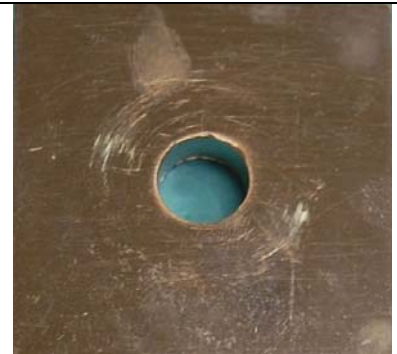


**Figure 11:** Electrochemical Impedance spectroscopy Bode plots of ASTM A470 and 7050-T74 alloy coated with Ecoline 3690 inhibitor in 200ppm Cl<sup>-</sup> solutions.

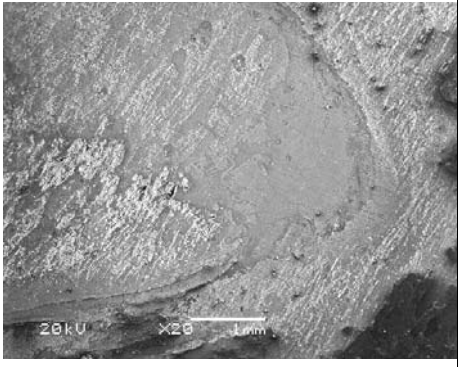
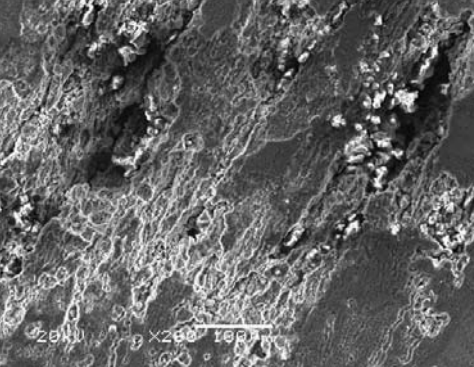
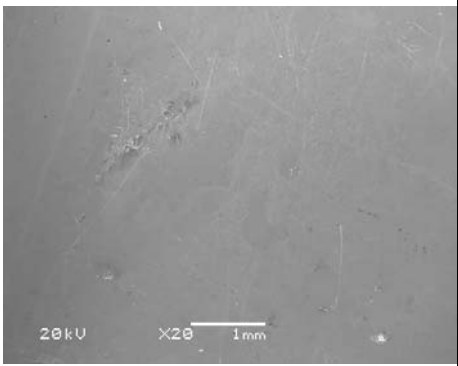
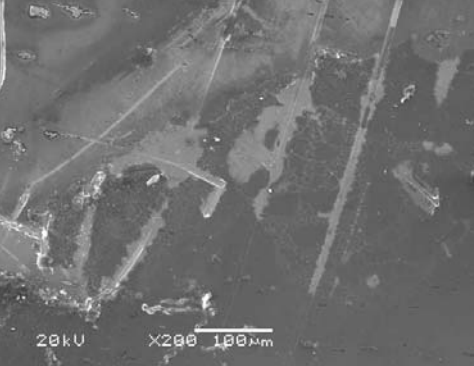
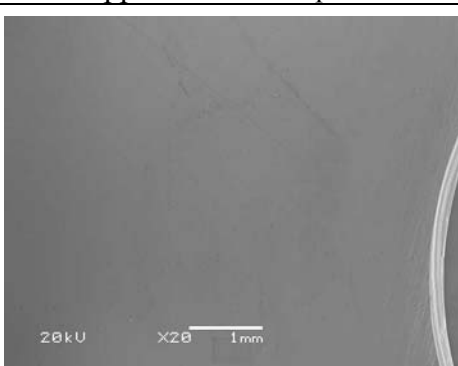
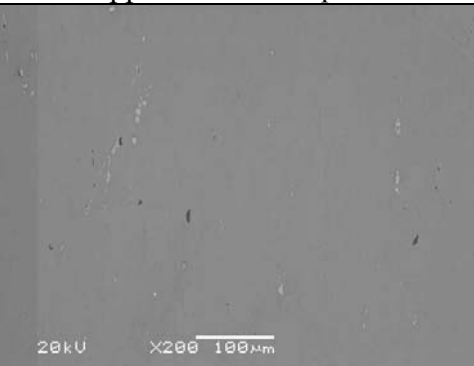


### Crevice Corrosion

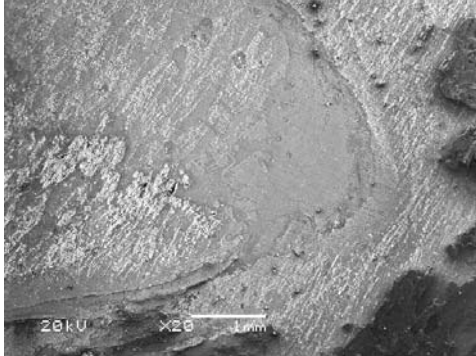
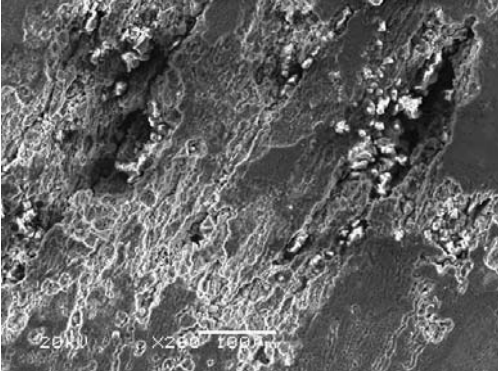
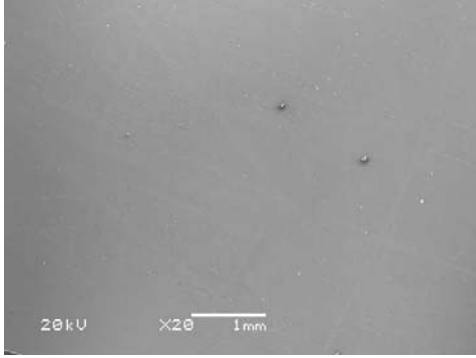
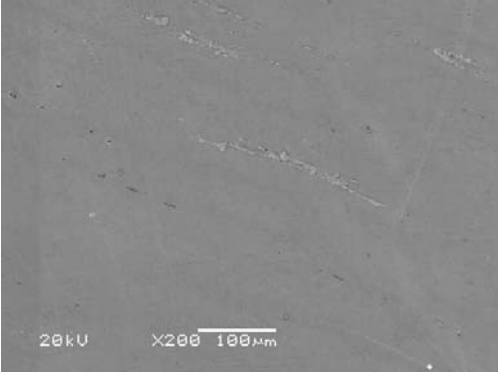
Figures 12-16 show photos of 7050-T74 aluminum alloy and ASTM A470 samples after 200 hours of alternate immersion in various solutions. The samples immersed in tap water and +200PPM Cl<sup>-</sup> show severe corrosion damage. The corrosion damage reduced with the addition of inhibitor to the environments (solutions). The passive film stability has improved the corrosion resistance for the inhibitor treated samples. Coated samples with Ecoline 3690 did not show any corrosion attacks, due to hydrophobic nature of this inhibitor, aggressive species could not wet the surface, therefore results on an excellent corrosion protection.

	200 ppm Cl <sup>-</sup>		1% VCI, + 200ppm Cl <sup>-</sup>
	Tap water		5% VCI, + 200ppm Cl <sup>-</sup>

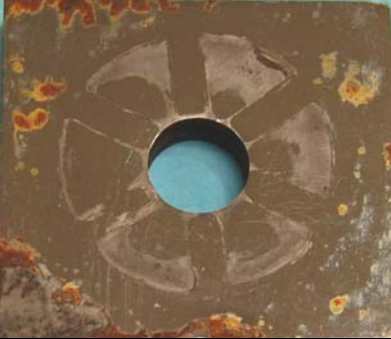




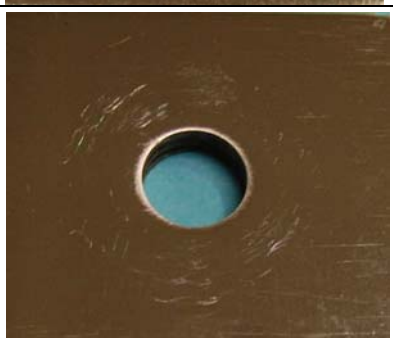
**Figure 12:** Crevice corrosion tests on 7050-T74 alloy in alternate immersion for 200 hours.

Cycles	+200ppm Cl-	+200ppm Cl-
200		
	+200ppm Cl- +1.0%VpCI 337	+200ppm Cl- +1.0%VpCI 337
200		
	+200ppm Cl- +5.0%VpCI 337	+200ppm Cl- +5.0%VpCI 337
200		

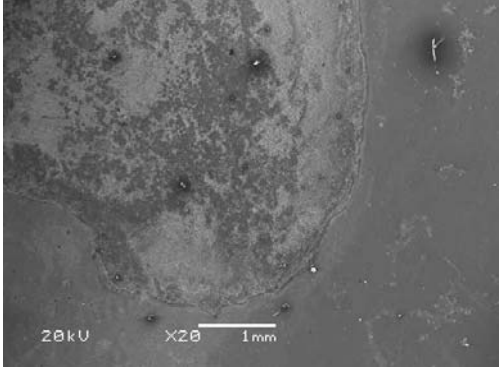
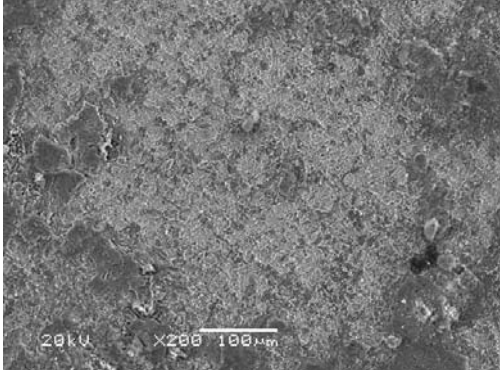
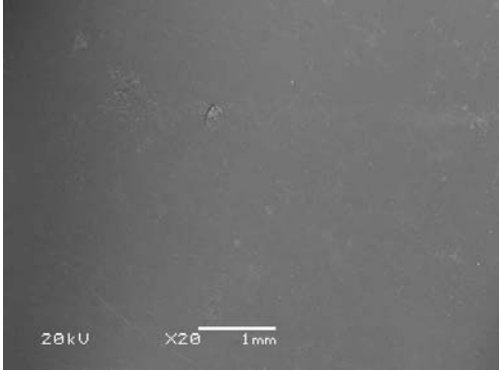
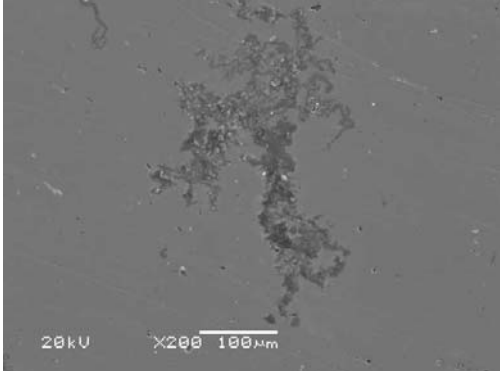
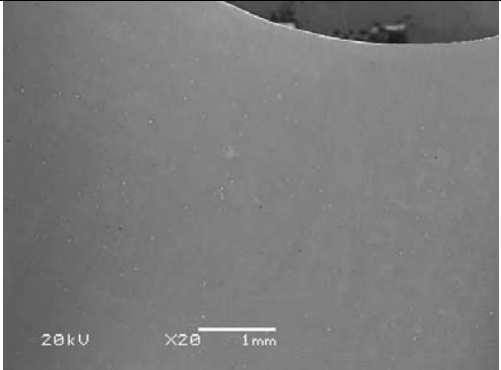
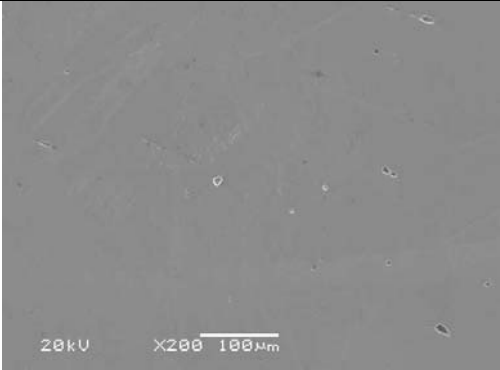
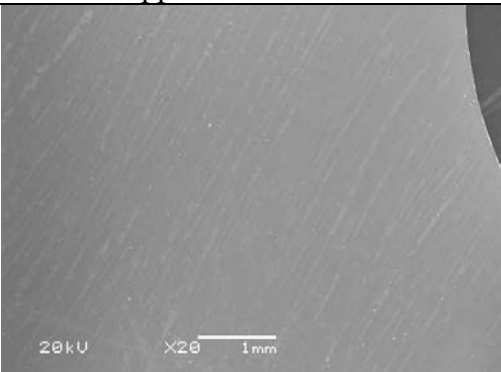
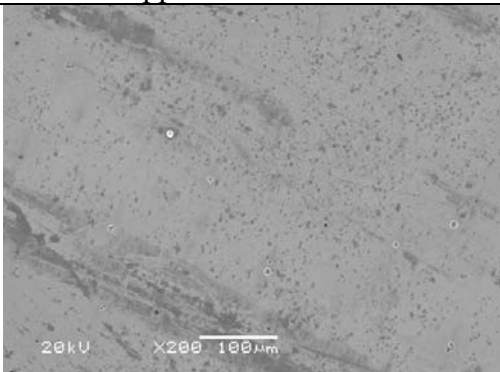
**Figure 13:** SEM micrographs of the surface of 7050-T74 after crevice corrosion tests in water solution with 1.0% VCI 337 inhibitor per ASTM G44.

Cycles	+200ppm Cl <sup>-</sup>	+200ppm Cl <sup>-</sup>
200		
	+200ppm Cl <sup>-</sup> /Ecoline 3690	+200ppm Cl <sup>-</sup> /Ecoline 3690
200		

**Figure 14:** SEM micrographs of the surface of 7050-T74 after crevice corrosion tests in 200ppmCl<sup>-</sup> solution after being coated with Ecoline 3690 inhibitor per ASTM G44.

	200ppm Cl <sup>-</sup>		1% VCI, + 200ppm Cl <sup>-</sup>
	Tap water		5% VCI, + 200ppm Cl <sup>-</sup>
	Ecoline VCI, + 200ppm Cl <sup>-</sup>		Ecoline VCI, + water

**Figure 15:** Crevice corrosion tests on ASTM A470 in alternate immersion for 200 hours.

Cycles	+200ppm Cl <sup>-</sup>	+200ppm Cl <sup>-</sup>
200		
	+200ppm Cl <sup>-</sup> +1.0%VpCI 337	+200ppm Cl <sup>-</sup> +1.0%VpCI 337
200		
	+200ppm Cl <sup>-</sup> +5.0%VpCI 337	+200ppm Cl <sup>-</sup> +5.0%VpCI 337
200		
	+200ppm Cl <sup>-</sup> +Ecoline 3690	+200ppm Cl <sup>-</sup> +Ecoline 3690
200		

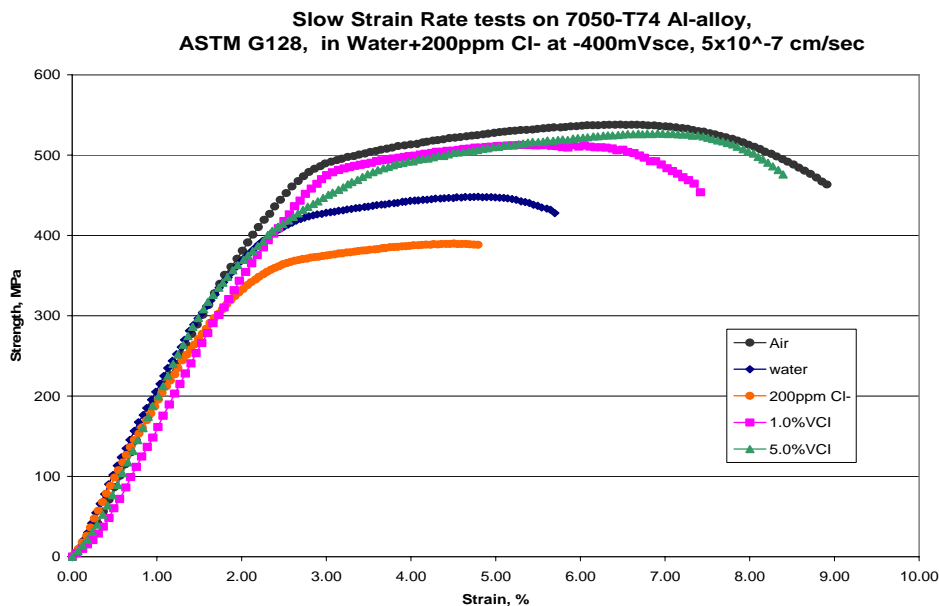
**Figure 16:** SEM micrographs of the ASTM A470 surface after crevice corrosion tests in +200ppm Cl<sup>-</sup> solution with 5.0% VCI 337 inhibitor per ASTM G44.

## Stress Corrosion Cracking

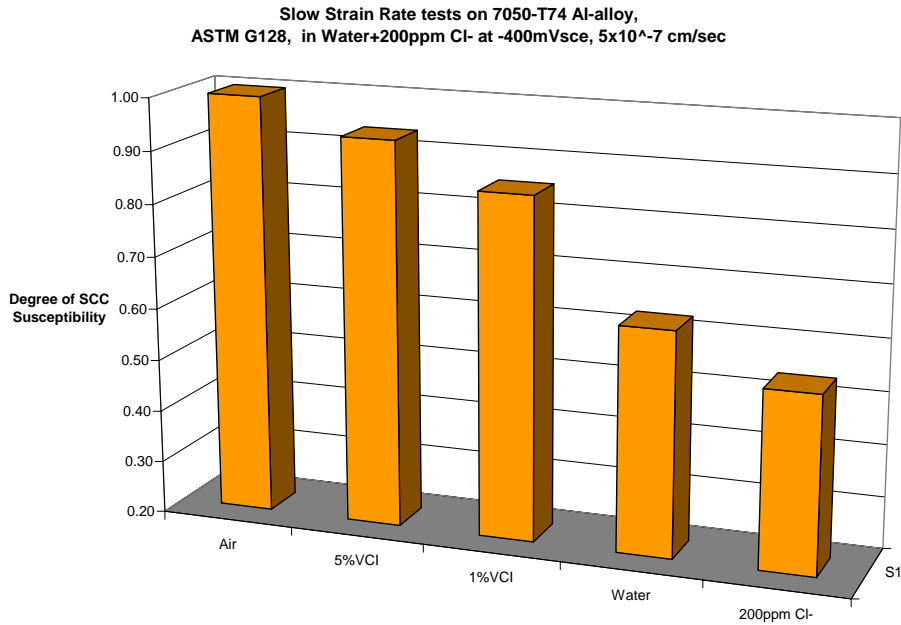
Susceptibility to SCC was determined for these two alloys using the slow strain rate test per ASTM G128. At applied potentials close to the passive film breakdown potential, a noticeable increase in susceptibility was seen for the samples tested without inhibitor. The greatest reduction in degree of susceptibility is seen around  $-200\text{mVsce}$  for the ASTM A470 steel and around  $-400\text{mVsce}$  for the 7050-T74 Al-alloy. Figures 17-18 show the SCC test results for 7050-T74 Al-alloy, as demonstrated addition of 5.0% VpCI 337 inhibitor retarded the SCC of this alloy.

Figure 19 shows the fatigue crack growth rate for the 7050 alloy in different solutions, as demonstrated the addition of 5.0% inhibitor lowered the fatigue crack growth rate.

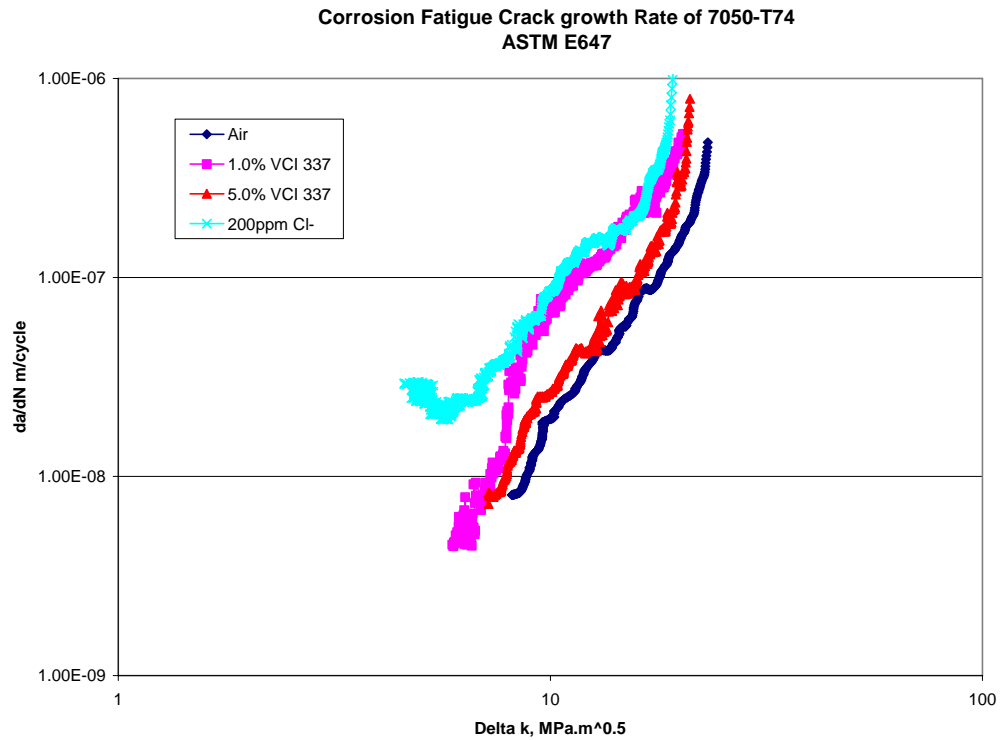
Figures 20-22 show the SEM fractographs for the SCC. These micrographs demonstrate greater SCC susceptibility for samples tested in solutions without inhibitor. Examination of the failed samples revealed some damage for all aluminum alloys in both testing conditions at the more aggressive potentials ( $-400\text{ mV}$ ). The SEM photos for the 7050 alloy showed some SCC attack and pitting corrosion at the edges. Figures 23-25 show the SCC test results for ASTM A470 steel. ASTM A470 steel showed morphology with intergranular attack for the samples tested in unprotected solutions. Figure 26 shows a comparison of the SCC susceptibility of ASTM A470 and 7050 in different solutions. In the presence of 5.0% VpCI 337 inhibitor, however, it showed mainly ductile overload failure with significantly less localized corrosion damage except at aggressive anodic potentials higher than  $-200\text{ mVsce}$  (Figures 27-29). Samples tested in the coating of Ecoline 3690 inhibitor showed mainly ductile overload failure with significantly less localized corrosion damage at applied potential of  $-200\text{ mVsce}$ . The slow strain rate tests showed that the protection afforded by both inhibitors (VpCI 337 and Ecoline 3690) are noticeable in the anodic potential range. Corrosion fatigue tests on 7050 Al-alloy showed that the fatigue crack growth rate in the presence of inhibitor is more similar to inert environments. Fatigue crack growth tests (ASTM E647) were conducted in 5% VpCI 337 solution and showed no evidence of crack arrest effects in  $+200\text{ppm Cl}^-$  solution, mainly due to less corrosion product formation.



**Figure 17:** The slow strain rate test results for 7050-T74 after SCC tests in different solutions.

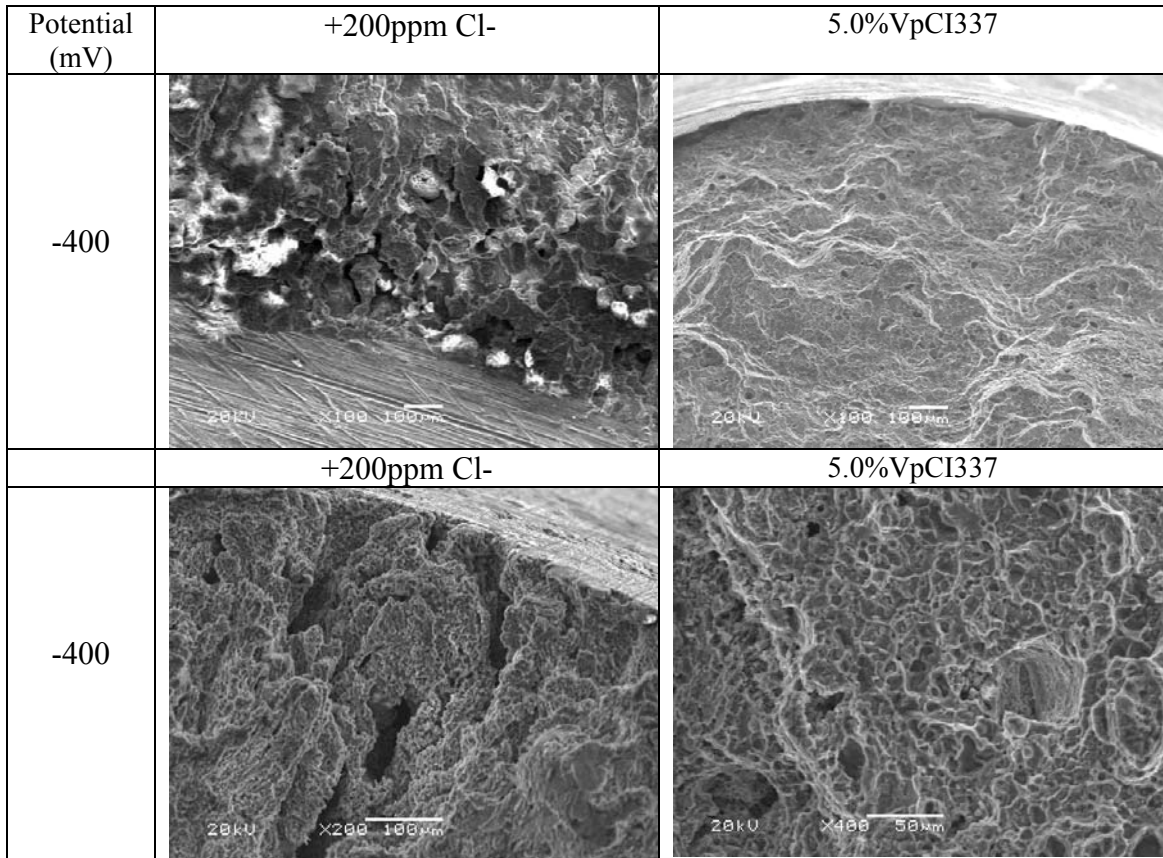


**Figure 18:** The SCC degree of susceptibility for 7050-T74 after SCC tests in different solutions.

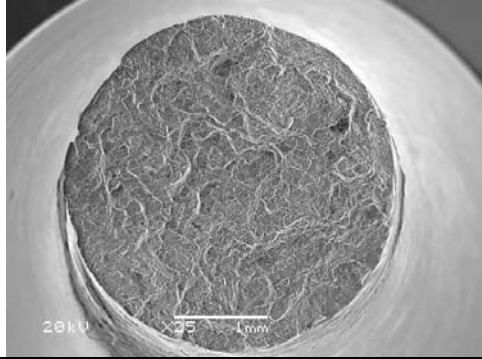
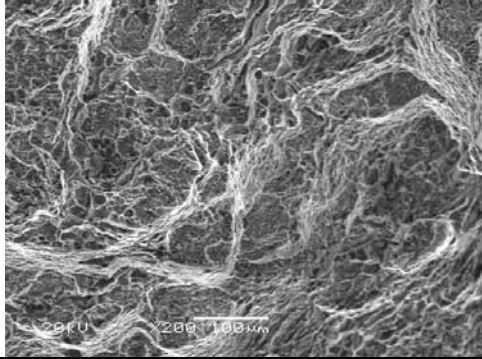
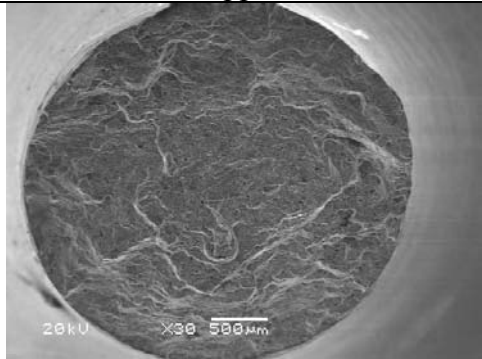
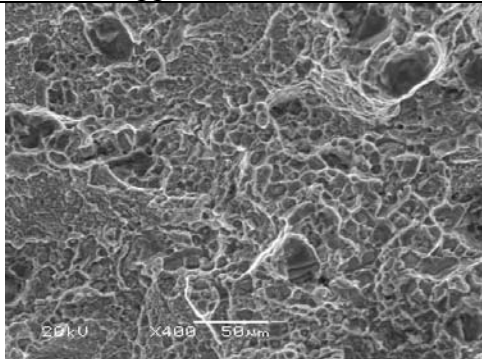


**Figure 19:** The fatigue crack growth rate for 7050-T74 in different solutions.

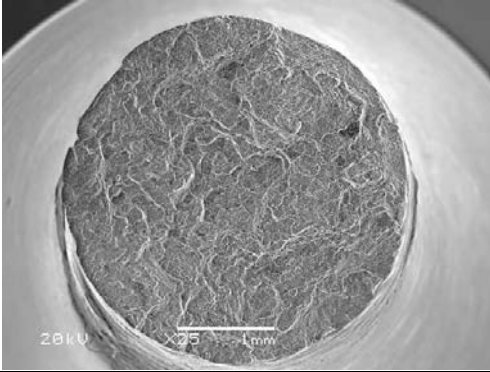
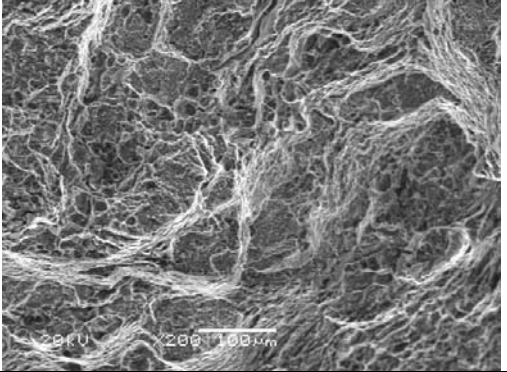
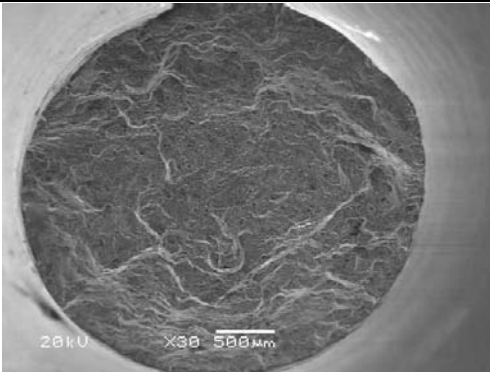
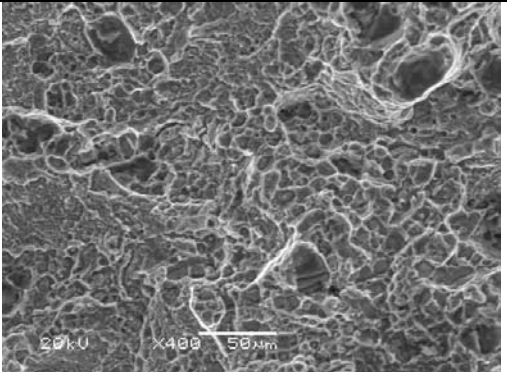




**Figure 20:** SEM micrographs of the fracture surface for 7050-T74 after SCC tests in different electrochemical conditions.

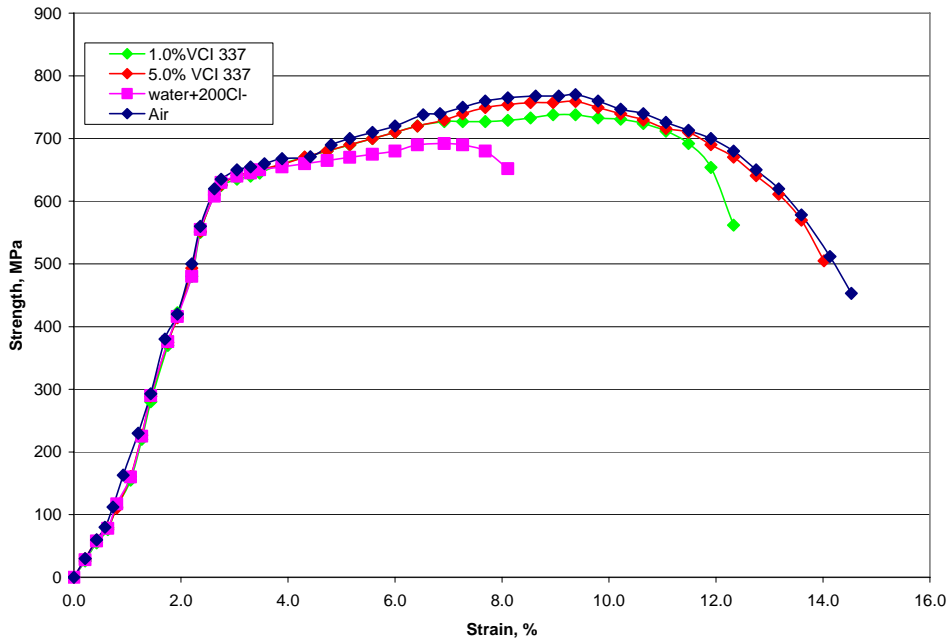
Potential (mV)	Water/Ecoline 3690	Water/Ecoline 3690
-400		
	+200ppm Cl-	+200ppm Cl-/Ecoline 3690
-400		

**Figure 21:** SEM micrographs of the fracture surface for 7050-T74 after SCC tests in water solution and Ecoline 3690 inhibitor coating per ASTM G128.

Potential (mV)	Tap water/Ecoline 3690	Water/Ecoline 3690
-400		
	+200ppm Cl-	+200ppm Cl-/Ecoline 3690
-400		

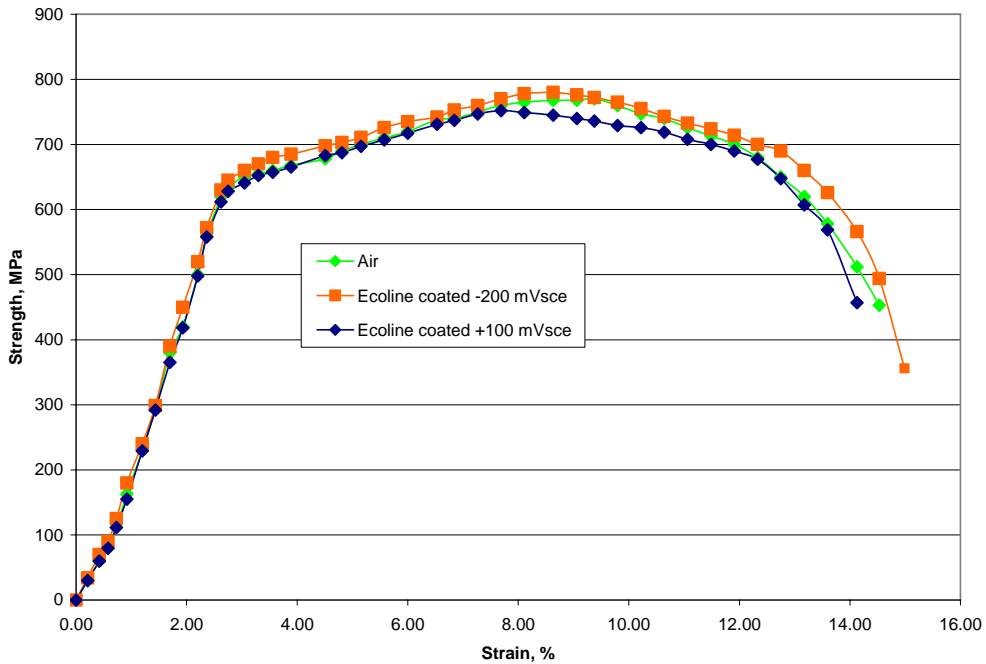
**Figure 22:** SEM micrographs of the fracture surface for 7050-T74 after SCC tests in water solution and Ecoline 3690 inhibitor coating per ASTM G128.

Slow Strain Rate tests on ASTM A470 Steel,  
ASTM G128, in Water+200ppm Cl- at -200mVsce,  $5 \times 10^{-7}$  cm/sec



**Figure 23:** The slow strain rate test results for ASTM A470 steel after SCC tests in different solutions. 5% VpCI 337 behaved similar to an inert environment.

Slow Strain Rate tests on ASTM A470 Steel,  
ASTM G128, in Water+200ppm Cl-,  $5 \times 10^{-7}$  cm/sec



**Figure 24:** The slow strain rate test results for the inhibitor coated ASTM A470 steel, showing a very effective SCC inhibition.

Slow Strain Rate tests on ASTM A470 Steel,  
ASTM G128, in Water+200ppm Cl<sup>-</sup> at -200mVsce, 5x10<sup>-7</sup> cm/sec

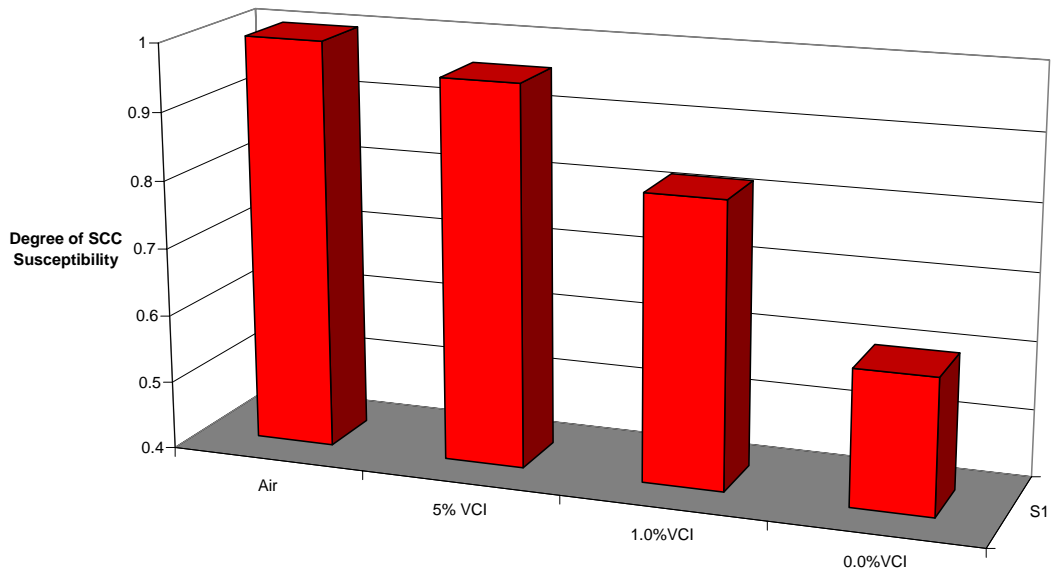


Figure 25: SCC susceptibility of ASTM A470 using the slow strain rate technique.

Slow Strain Rate tests on 7050-T74 Al-alloy(-400mVsce) and ASTM A470 (-200mVsce), ASTM G128, in Different Solutions at , 5x10<sup>-7</sup> cm/sec

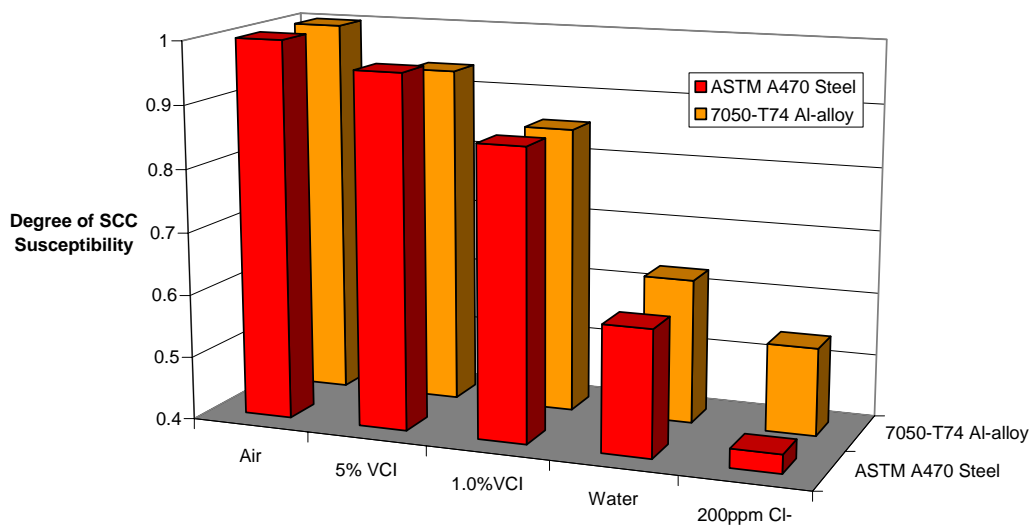
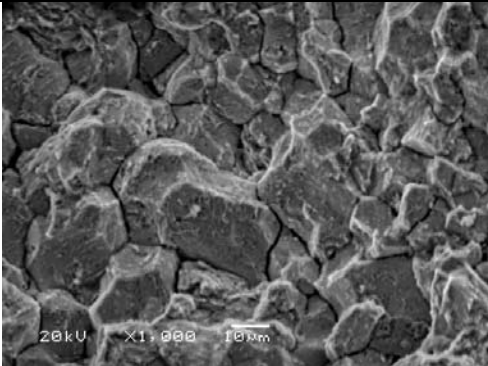
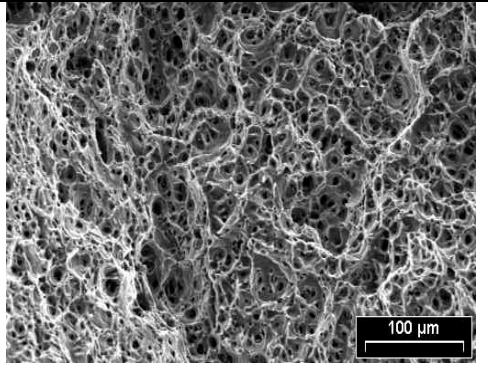
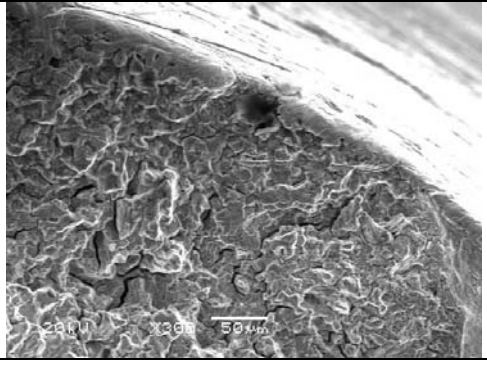
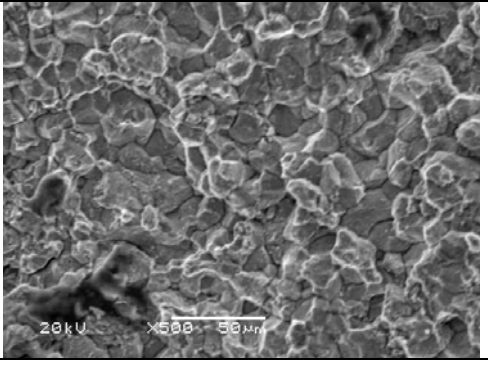
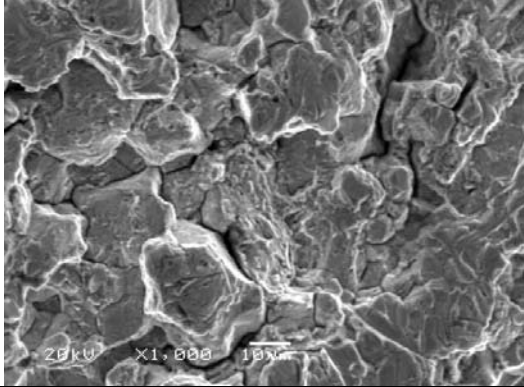
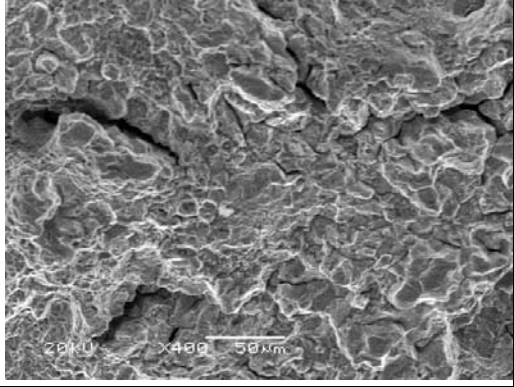
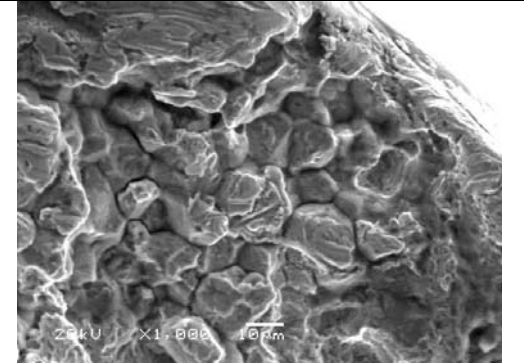
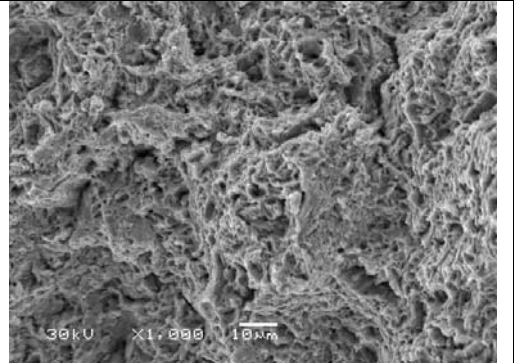


Figure 26: Comparison of SCC susceptibility of ASTM A470 and 7050 in different solutions.

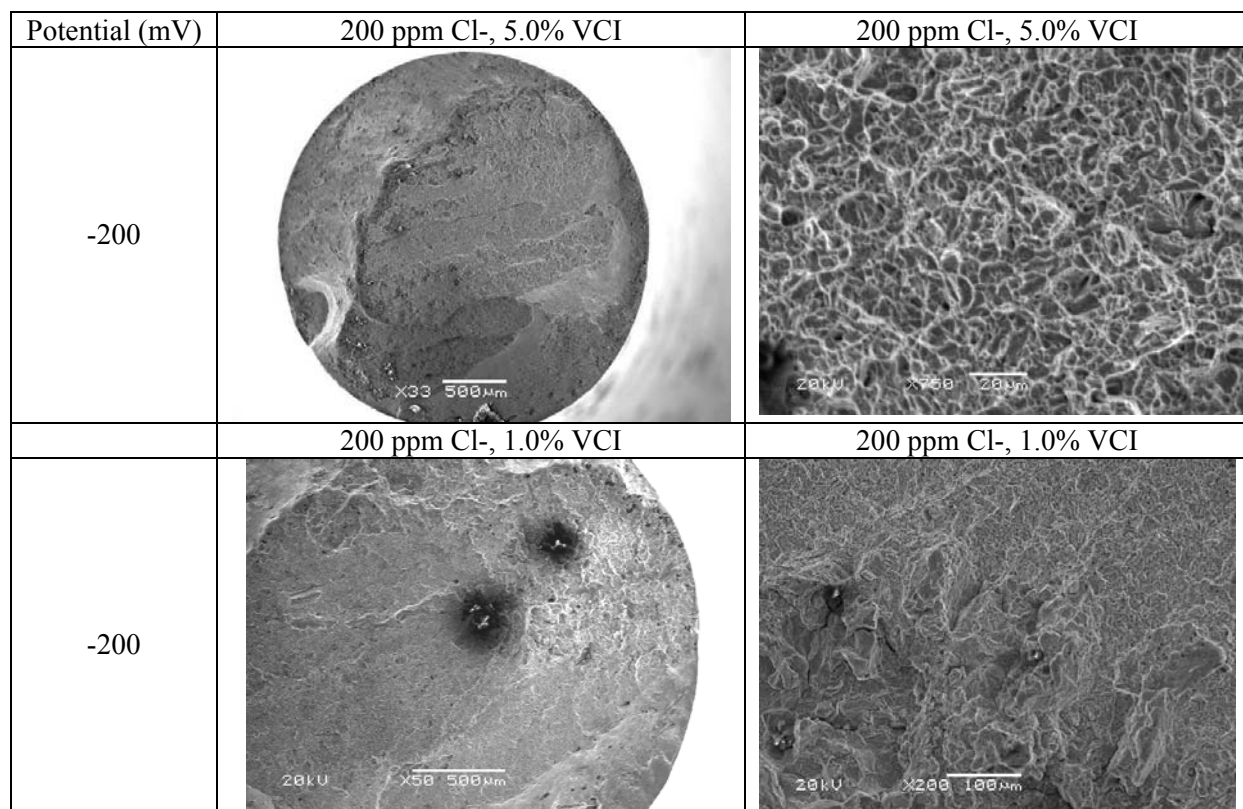
Potential (mV <sub>sce</sub> )	200ppm Cl <sup>-</sup>	Air
-200		
-200		

**Figure 27:** SEM micrographs of the fracture surface for ASTM A470 after SCC tests in different electrochemical conditions.

Potential (mV)	water	1.0%VCI
-200		
	200 ppm Cl-	5.0%VCI
-200		

**Figure 28:** SEM micrographs of the fracture surface for ASTM A470 after SCC tests in different electrochemical conditions.



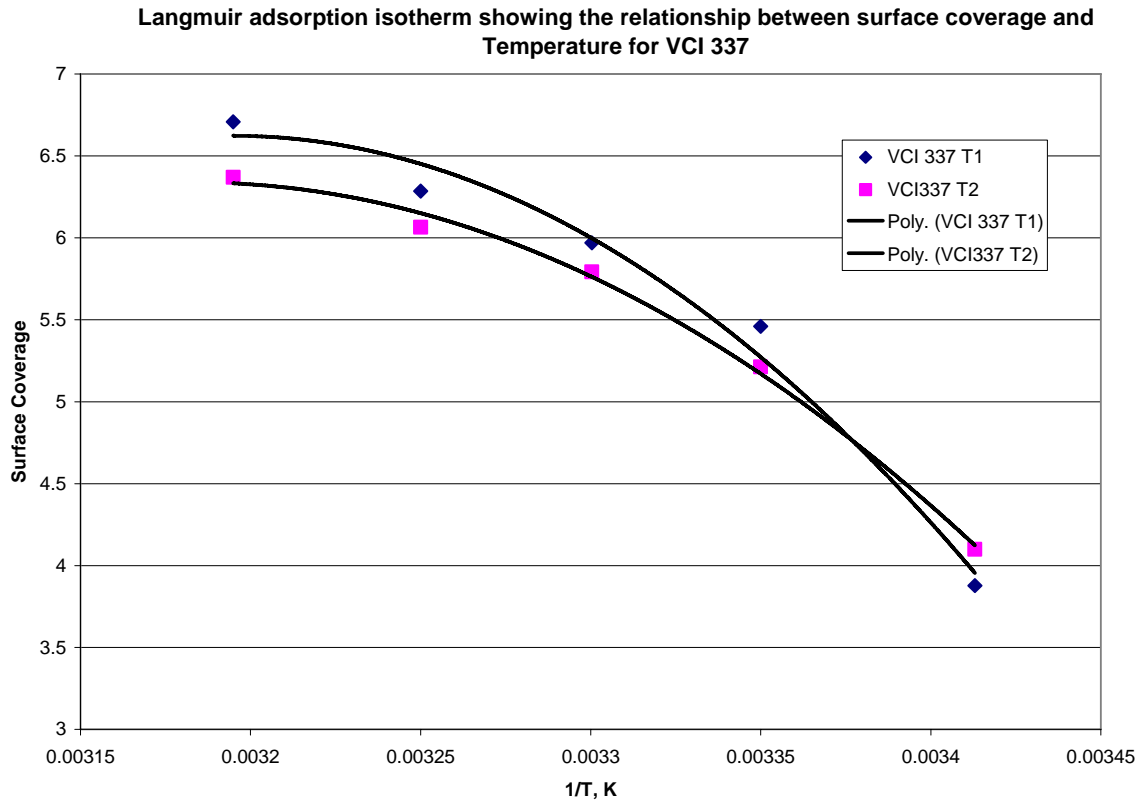


**Figure 29:** SEM micrographs of the fracture surface for ASTM A470 after SCC tests in different electrochemical conditions.

### Verification of the Inhibition Mechanism

The corrosion inhibition mechanism of VpCI 337 inhibitor was investigated using the data acquired from the EIS tests. EIS, when modeled correctly, is a powerful tool for the analysis of complex electrochemical systems. A modified Randles model was used to obtain the polarization resistance ( $R_p$ ) values. The Bode plots show that VCI increases the polarization resistance of both alloys (Figures 5-8 and Tables 9-10) with higher inhibitor concentrations resulting in higher  $R_p$  values. The increased polarization resistance can be attributed to the adsorption of inhibitor molecules on the metal surfaces. The addition of inhibitor has increased the  $R_p$  value from 2.8 k $\Omega$  for ASTM A470 in the blank solution (0 ppm concentration) to 220 k $\Omega$  for 1.0% VCI, 766 k $\Omega$  for 5.0% VCI in solution (Table 10). The high  $R_p$  value is due to the progressive adsorption of inhibitor molecules and film formation on the metal surface. The data obtained from the EIS experiment best fit the Langmuir adsorption isotherm, where  $\ln(\text{Concentration})$  vs.  $[\ln \theta - \ln(1 - \theta)]$  resulted in good linearity. The important thermodynamic values (changes in enthalpy of adsorption and changes in free standard energy of adsorption) can be obtained with adsorption isotherms and classical thermodynamics. The value of  $\Delta G_{ad}$  could be used to identify of the adsorption mechanism. In chemisorption (chemical adsorption),  $\Delta G_{ad}$  is usually much higher than physisorption (physical adsorption). The criterion for chemisorption varies, for example, Bridka has suggested that chemisorption requires about -100 kJ/mol energy, whereas Metikos-Hukovic believes that chemisorption needs about -40 kJ/mol energy [6-8]. Still others assert that physisorption requires energy between -5 to -20 kJ/mol [7]. The analysis on the VpCI 337 inhibitor showed the enthalpy of adsorption to be about -14 to -18 kJ/mol (Figure 30); this

suggests that this product is borderline between a strong physisorption and a weak chemical adsorption to the metal surface. Generally chemisorption makes strong bonding between the inhibitor and the surface of the substrate resulting in a more stable protective film. But, the majority of corrosion damage to turbo-machinery systems occurs during shutdown period due to chemistry changes and stagnant condition in localized areas; therefore, a strong physisorption corrosion inhibitor will provide satisfactory protection.



**Figure 30:** Langmuir adsorption isotherm showing the relationship between surface coverage and VCI concentration on the surface of the ASTM A470 steel.

## CONCLUSIONS

A comprehensive investigation was undertaken to characterize the corrosion behavior of turbo-machinery systems in vapor phase corrosion inhibitor. Effectiveness of the inhibitor was confirmed with electrochemical impedance spectroscopy and cyclic polarization in room temperature and elevated temperature studies. As well, identification of the adsorption mechanism and corrosion activation energy was explored. The data acquired from EIS tests showed that inhibitor adsorption to these alloy surfaces fits with the Langmuir adsorption isotherm; the enthalpy of adsorption is about -14 to -18 kJ/mol, suggesting that this product is a strong physisorption or at least a relatively weak chemisorption compound.

Cyclic polarization behavior for samples in the vapor phase inhibitor showed a shift in the passive film breakdown potential by roughly +500 mV. This increase in the passive film range

will improve localized corrosion resistance. Crevice corrosion test results showed improved corrosion inhibition behavior compared with unprotected samples. The SCC susceptibility degree from the stress corrosion cracking studies showed significant reduction in SCC susceptibility in environments with added VpCI. Furthermore, ductile overload failure mode was observed for the alloys tested in the 5% VpCI 337 and Ecoline 3690 inhibitor solution. In summary, both VpCI 337 and Ecoline 3690 inhibitors provide an effective corrosion protection for both ASTM A470 and 7050 alloys during the shutdown period for the blades and discs in low pressure steam turbines.

**ACKNOWLEDGEMENT:** The authors would like to express their appreciation to the W.M. Keck Foundation, AHPMC and Cortec Corp. for their sponsorship of this project.

## REFERENCES

- [1] H. McCloskey, R. B. Dooley and W. P. McNaughton, Turbine Steam Path Damage: Theory and Practice, Vol. 1 and 2. EPRI, Palo Alto, CA: 1999.
- [2] G. Engelhardt and D. Macdonald, Development of Code to Predict Stress Corrosion Cracking and Corrosion Fatigue of Low Pressure Turbine Components. EPRI, Palo Alto, CA: February 2004. 1004190.
- [3] G. Engelhardt and D. Macdonald, Corrosion Science, 46, 2755: 2004.
- [4] M. R. Saleh, A.M. Shams El Din, Corrosion Science, 12 (1981) 688.
- [5] M. L. Free, A new corrosion inhibition model for surfactants that more closely accounts for actual adsorption than traditional models that assume physical coverage is proportional to inhibition, Corrosion Science, In Press, Corrected Proof, 10 May 2004.
- [6] M. Lagrenée, B. Mernari, M. Bouanis, M. Traisnel and F. Bentiss, Study of the mechanism and inhibiting efficiency of 3,5-bis(4-methylthiophenyl)-4H-1,2,4-triazole on mild steel corrosion in acidic media, Corrosion Science, Vol 44, Issue 3, March 2002.
- [7] W. Durine, R. D Marco, A. Jefferson, and B. Kinsella, JES, 146 (5) 1751-1756 (1999)
- [8] R. Gasparac, C. R. Martin and E. Stupnisek-Lisac, In situ Studies of Imidazole and its Derivatives as Copper Corrosion Inhibitors, Journal of The Electrochemical Society, 147 (2) 548-551 (2000).